Electrochemical Society

99, No. 6 1952

UNIV. OF MICHIGAN
SEP 4 1952
EAST ENGINEERING
LIBRARY

1902—FIFTIETH ANNIVERSARY—1952

Storage Battery Issue

Electrolytic Aids to INSECTICIDE MANUFACTURE

Chlorine and caustic soda, products of the electrolytic industry, are essential to insecticide manufacture.

Uniformly high quality **GLC Graphite Anodes** are equally important to the chlorine and caustic soda production of many leading electrochemical manufacturers. The performance of **GLC Graphite Anodes** in electrolytic cell operations is unsurpassed.

ELECTRODE DIVISION

Great Lakes Carbon Corporation

Niagara Falls, N. Y. GLC Morganton, N. C.

Courtesy Piper Aircraft

Graphite Anodes, Electrodes and Specialties

Sales office: Niagara Falls, N. Y. • **Other offices:** New York, N. Y., Chicago, Ill., Pittsburgh, Pa.

Sales Agents: J. B. Hayes Company, Birmingham, Ala., George O'Hara, Wilmington, Cal.

Journal of the

Electrochemical Society

SEPTEMBER, 1952 VOLUME 99 • NUMBER 9

CONTENTS

Anniversary Features

Packages of Power—Editorial. *George W. Vinal* 229C
The Anniversary Issue on Storage Batteries 233C–254C
Ten articles by *J. C. White, E. Willihnganz, H. C. Riggs, Upton B. Thomas, C. H. Endress, C. C. Rose, A. C. Zachlin, Fayette C. Anderson, Sven Bergstrom, G. B. Ellis, H. Mandel, D. Linden, and Samuel Eidensohn.*

Feature Section

The Teaching of Electrochemistry (Round-Table Discussion). *R. B. Mears* 255C

Technical Papers

Positive-Plate Self-Discharge in the Lead-Acid Cell. *John J. Lander* .. 339
An Electrochemical Evaluation of Manganese Dioxide for Dry Battery Use. *N. C. Cahoon* 343
The Electrodeposition of Silver on an Iron-Nickel Alloy for a Glass-to-Metal Seal Arrangement. *R. T. Foley, R. D. Alvord, and J. K. Easley* 349
Electrolytic Determination of Tin and Tin-Iron Alloy Coating Weights on Tin Plate. *C. T. Kunze and A. R. Willey* 354
Role of Crystal Orientation in the Oxidation of Iron. *Earl A. Gulbransen and Roswell Ruka* 360

Current Affairs

Plant Trips and Other Plans for Montreal Meeting 257C
News Notes 259C
Section and Division News 260C
Personals 260C
New Members 260C
Letter to the Editor 261C
Book Reviews 263C
Literature from Industry 264C
Recent Patents 266C
Employment Situations 266C

EDITORIAL STAFF

R. M. BURNS, *Chairman*

NORMAN HACKERMAN, *Technical Editor* RUTH G. STERNS, *Assistant Editor* F. L. LAQUE, *Business Manager*
CECIL V. KING, *Associate Editor* MARY F. MURRAY, *Assistant Editor* U. B. THOMAS, *News Editor*

DIVISIONAL EDITORS: M. A. STREICHER, *Corrosion;* ABNER BRENNER, *Electrodeposition;* N. C. CAHOON, *Battery;* H. C. FROELICH, *Electronics;* W. C. GARDINER, *Industrial Electrolytic;* S. J. SINDEBAND, *Electrothermic;* JOHN J. CHAPMAN, *Electric Insulation;* L. B. ROGERS, *Theoretical;* SHERLOCK SWANN, JR., *Electro-Organic.*

REGIONAL EDITORS: JOSEPH A. SCHULEIN, *Pacific Northwest;* J. C. SCHUMACHER, *Los Angeles;* O. W. STOREY, *Chicago;* G. W. HEISE, *Cleveland;* PAUL S. BRALLIER, *Niagara Falls;* OLIVER OSBORN, *Houston;* EARL A. GULBRANSEN, *Pittsburgh;* J. W. CUTHBERTSON, *Great Britain;* T. L. RAMA CHAR, *India.*

ADVERTISING OFFICE: Jack Bain, Mgr., 545 Fifth Ave. Suite 1109, New York 17, N.Y. Telephone: Murray Hill 2-3345.

Published monthly by The Electrochemical Society, Inc., Mt. Royal and Guilford Aves., Baltimore 2, Md., combining the JOURNAL and TRANSACTIONS OF THE ELECTROCHEMICAL SOCIETY. Editorial Office: 235 W. 102nd St., New York 25, N. Y. Business Office: Mt. Royal and Guilford Aves., Baltimore 2, Md., or 235 W. 102nd St., New York 25, N. Y. Statements and opinions given in articles and papers in the JOURNAL OF THE ELECTROCHEMICAL SOCIETY are those of the contributors, and The Electrochemical Society assumes no responsibility for them. Subscription: $8.50 to members, $12.00 to nonmembers. Single copies $1.00 to members, $1.25 to nonmembers. Copyright 1952 by The Electrochemical Society, Inc. Entered as second-class matter November 15, 1947, at the Post Office at Baltimore, Md., under the act of August 24, 1912.

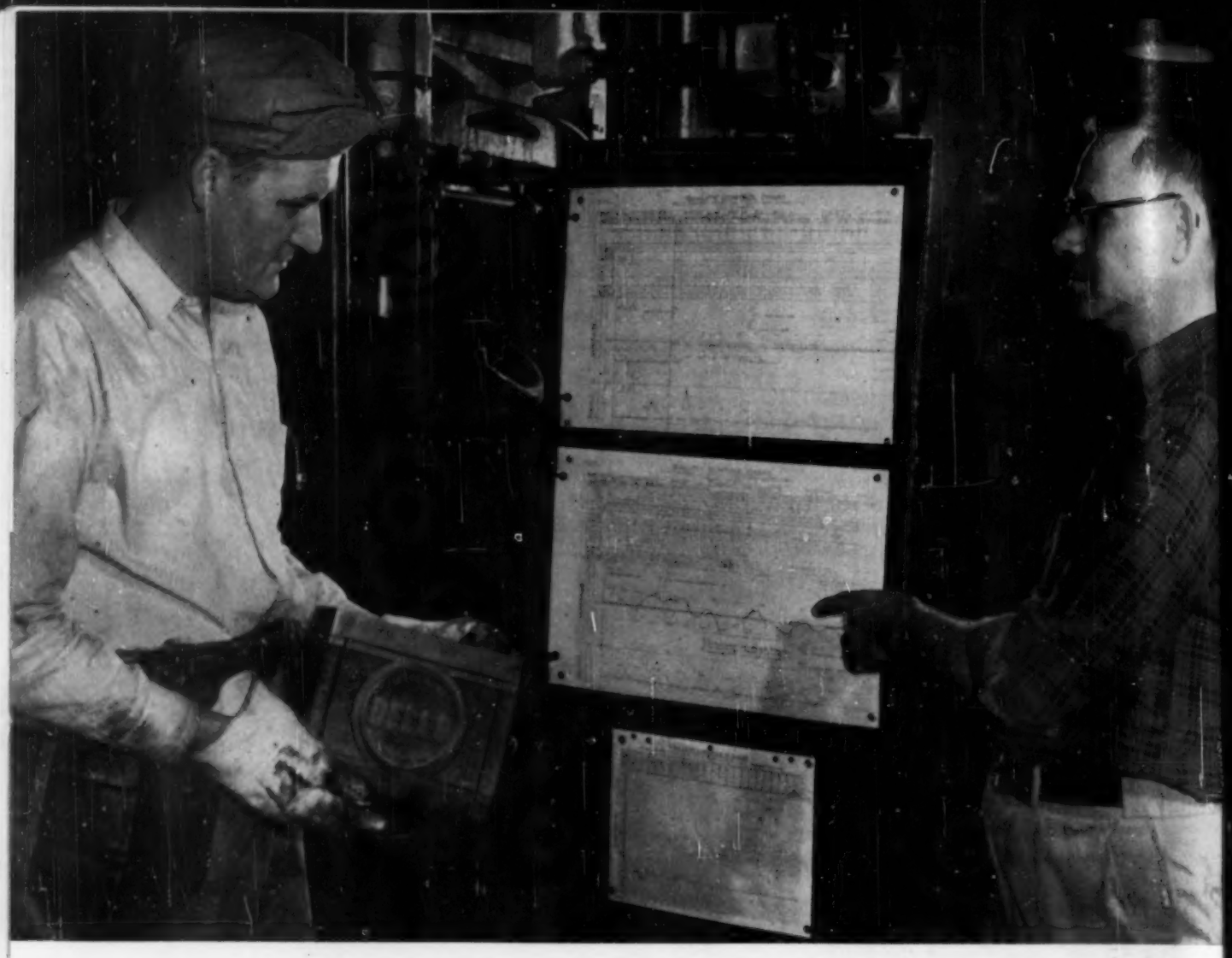

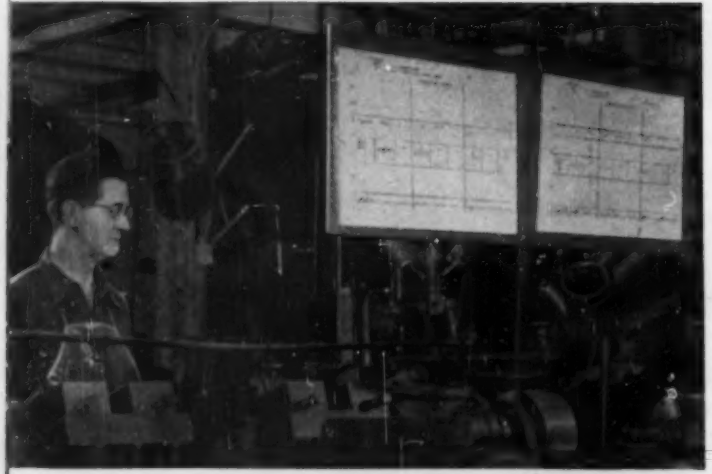

CHARTING A COURSE

to higher quality

The pictures on this page show dramatically how Delco-Remy charts a course to higher quality in the manufacture of automotive electrical equipment. All along the production line, Delco-Remy products are subjected to rigid inspections and tests. The many quality control charts reflect the high standards which have been a Delco-Remy tradition for more than 50 years.

DELCO-REMY

DIVISION · GENERAL MOTORS CORPORATION
ANDERSON, INDIANA

AUTOMOTIVE, TRACTOR AND MARINE ELECTRICAL EQUIPMENT

Positive-Plate Self-Discharge in the Lead-Acid Cell[1]

JOHN J. LANDER

Naval Research Laboratory, Washington, D. C.

ABSTRACT

Specific gravity changes on stand in lead-acid cells having 12 per cent antimonial grids were followed for 46 months. Self-discharge at the positive plate was found to occur at rates comparable to negative-plate self-discharge. It appears to proceed primarily through oxidation of the antimony in the grid by the PbO_2 in the plate. Hydrogen gas was found to reduce PbO_2 in sulfuric acid.

INTRODUCTION

As part of an experimental program to determine the effects of long-term wet storage on lead-acid cells, a number of cells were allowed to stand under sulfuric acid of various gravities. The decreases in gravity were measured from time to time, and it is believed that the results obtained, together with other information, may be interpreted to show the primary cause of self-discharge at positive plates with antimonial grids.

Vinal (1) regards positive-plate self-discharge as occurring as the result of a reaction which is the same as the cell reaction:

$$PbO_2 + Pb + 2H_2SO_4 = 2PbSO_4 + 2H_2O. \quad (I)$$

Zachlin has done extensive work on the general subject, and his papers (2, 3) contain a substantial bibliography. Positive-plate self-discharge is described in his work as being due to "local action" and no attempt is made to define it further.

Greenburg and Caldwell (4) studied positive-plate self-discharge, and their experiments appear to lay it nearly quantitatively to three causes: first, that which results in grid corrosion according to equation (I); second, that represented by the empirical equation:

$$PbO_2 + H_2SO_4 \rightarrow PbSO_4 + H_2O + \tfrac{1}{2}O_2; \quad (II)$$

and third, chemical reaction of unformed PbO:

$$PbO + H_2SO_4 = PbSO_4 + H_2O. \quad (III)$$

EXPERIMENTAL

Sixteen aircraft cells, having a rated capacity of 16 amp-hr at the four-hour rate and having 12 per cent Sb grids, which had been received in the dry-charged condition, were given a freshening charge for several days and then cycled a few times to develop capacity. They were then discharged for 4½ hours at 4 amp and the electrolyte was dumped. Four groups of four cells each were filled with acid which was adjusted to specific gravities 1.385, 1.345, 1.290, and 1.245, respectively, after sufficient mixing with the spent acid retained after draining.[2] The cells were equipped with nonspill plastic caps so that evaporation was slow. Nevertheless, over the long periods of time involved, it was appreciable and watering was necessary. Sufficient time was allowed for diffusion mixing before making specific gravity measurements, which were made with an accuracy greater than necessary for subsequent calculations.

After 46 months one cell from each group was taken apart, and active material from positive and negative plates of each cell was analyzed using x-ray diffraction. Samples of active material from each plate of the 1.290 cell were analyzed by boiling in ammonium acetate solution and weighing the residue (metallic Pb, or PbO_2). Grid corrosion from one cell of each group (except the 1.290 group) was determined by stripping the corrosion product from the grids in boiling ammonium acetate solution and comparing their stripped weights with those for grids from a new, freshly charged cell similarly stripped.

RESULTS AND CONCLUSIONS

The average gravity for each group of cells as a function of time is shown in Fig. 1. From these data, and from the volume of electrolyte in the cell (240 cc), the weights of H_2SO_4 used up were calculated, and the values obtained are given in Table I together with the original weight of H_2SO_4 present.

These cells have three positive plates and four negative plates. The original weight of one positive grid $\cong$58 g, the weight of PbO_2 in one positive plate $\cong$69 g, and the weight of Pb in one negative plate $\cong$49 g. The original discharge would have left 130 g Pb and 131 g PbO_2 in each cell and complete reaction of these amounts of active materials would require 116 g of H_2SO_4. The values for acid consumption given in Table I are in error to the extent that increase in volume of the active material due to conversion to $PbSO_4$ was not taken into account. If this

[1] Manuscript received January 7, 1952.

[2] The discharged cells were refilled with new acid because previous work had indicated that if the acid was allowed to go to water on self-discharge, internal shorts might be expected to develop on charging after stand. No shorting was observed for these cells.

volume increase is considered, and if it is assumed that all the active material has reacted, then values can be calculated for the final specific gravities. If the measured values of final gravity are higher than those calculated, the active materials have not completely reacted, and an approximate correction can be applied to the original values of acid consumed. The corrected results are given in Table II. In addition, the specific gravity data of Fig. 1 have been converted to grams of acid used based on the corrected data, and the results are shown in Fig. 2.

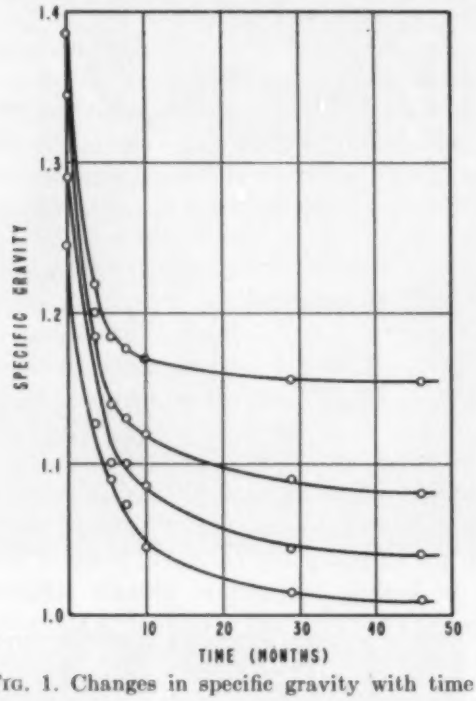

FIG. 1. Changes in specific gravity with time

TABLE I. *Weight of H_2SO_4 consumed per cell in 46 months*

Gravity groups	Wt of H_2SO_4 available, g	Wt consumed, g
1.385	161	103
1.345	142	112
1.290	118	103
1.245	98	94

Evidently self-discharge must have gone very nearly to completion at both plates.

The x-ray analyses of active material from the positive plate indicated substantially complete conversion to $PbSO_4$ in every case. The x-ray patterns for the negative-plate active material showed small amounts of lead remaining in each case. The chemical analysis of active materials from the 1.290 cell showed 97 per cent conversion of PbO_2 and 80 per cent conversion of Pb. These values calculate to 101 g of H_2SO_4 used up, a result in fair agreement with the corrected specific gravity data. The difference (105–101) may be due to sulfation of the negative grids and corrosion of metallic lead in the positive grids.

The results of measurements of grid corrosion are given in Table III. If the difference found above could be completely ascribed to corrosion of lead from the positive grids, then 8.5 g of lead would have been converted to $PbSO_4$. The remaining weight loss (assuming that the 1.290 cells corroded

TABLE II. *Comparison of calculated and measured final gravities*

Gravity group	Final gravity		Acid consumed (corrected)
	Calculated for complete reaction	Measured	
1.385	1.137	1.155	109
1.345	1.081	1.080	116
1.290	1.006	1.040	105
1.245	1.000	1.010	95

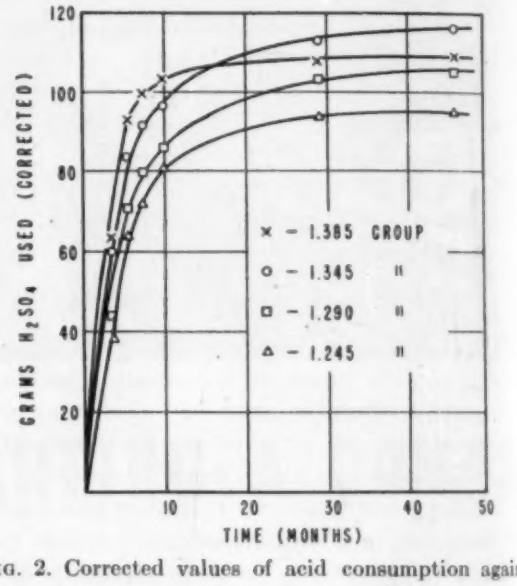

FIG. 2. Corrected values of acid consumption against time.

TABLE III. *Extent of grid corrosion*

Gravity group	Wt loss, g, for 3 positive grids*
1.385	13.5
1.345	21.0
1.245	22.5

* Original weight of stripped grids from dry-charged positives = 58 ± 0.5 g/grid.

to the same extent as the others) would then be due to corrosion of antimony.

The body of these calculated data cannot be considered quantitatively exact. For example, no account has been taken of conversion of negative grid metal to $PbSO_4$. Again, the final chemical state of corroded antimony is not definitely known; if the antimony exists in solution, it may have an effect on the measured specific gravities, but if it exists in part as solid antimony sulfate, then adjustments

would have to be made in much of the calculated data. Thus, the value of 8.5 g for lead corrosion at the positive grid would be lower and the antimony corrosion would be correspondingly greater. Nevertheless, the gravity changes are so nearly complete and the analyses show such a large amount of active material conversion that two definite conclusions can be drawn. First, self-discharge is very rapid in these cells until it approaches completion, and its over-all rate increases with acid strength. Second, while quantitative separation of self-discharge at both plates cannot be obtained, it is still evident that rates at the positives must be at least nearly as great as those at the negatives initially, because from Fig. 2 the whole self-discharge process approaches completion within 10 months. In fact, the x-ray data and chemical analysis show that over 46 months the self-discharge at the positive was appreciably greater than that at the negative. It is probably significant that these grids contained 12 per cent antimony, as will be indicated below.

As a check on the second conclusion, a positive plate, shown to be fully charged by x-ray analysis of a portion of the active material, was allowed to stand in excess acid of 1.200 specific gravity for 5 months. A sample of active material was then analyzed by the ammonium acetate method, and it was found that the PbO_2 was 62 per cent converted to $PbSO_4$.

Discussion

Self-discharge at the positive plate at such rates and to the extent shown in this work cannot be explained by any of the equations given in the introduction or by the sum of their effects. The cells were new, dry-charged cells which had been given a long freshening charge as well as a few cycles. It is possible that a small amount of unformed PbO may have been present, but the cells gave better than rated capacity after a few cycles and it is believed that PbO could not have been present in amounts sufficient to affect the argument to follow. The reaction (II) does not occur to any measurable extent by itself, because freshly electroformed PbO_2, removed from a plate, was allowed to stand in 1.300 acid for 5 months, and showed no $PbSO_4$ lines in its x-ray pattern at the end of this time. Reaction (I) undoubtedly does contribute to the self-discharge process, but even if all the grid corrosion took place by this reaction, not more than 24 g of PbO_2 per cell could have been converted as a result.

It is believed that positive-plate self-discharge is explained primarily by corrosion of antimony in the grids. Such corrosion has long been recognized (5), and Zachlin has shown (3) an appreciable increase in the rate of self-discharge at positive plates with increase in antimony content of the grids. The picture then is this: the PbO_2-$PbSO_4$ couple polarizes the grid up to the PbO_2-$PbSO_4$ potential at which the lead in the grid forms a film of PbO (6). This film has some protective action, and oxidation of the lead then becomes slow by comparison with oxidation of the antimony phase. Self-discharge proceeds by oxidation of antimony to one or both of its oxidation states, with corresponding reduction of PbO_2. The actual mechanism for self-discharge may be that proposed in an earlier paper (7), except that in this case electrons for the PbO_2 reduction are supplied chiefly by the antimony metal. The antimony ions then react with the solution phase.

Assuming that all the measured grid weight losses are accounted for by antimony, and using the data for the 1.345 group for example, the weight of PbO_2 reacted can be calculated using the reactions:

$$2Sb + 3PbO_2 + 6H_2SO_4 = 2Sb^{+++} + 3PbSO_4 + 6H_2O + 3SO_4^{=} \quad (IV)$$

and

$$2Sb + 5PbO_2 + 10H_2SO_4 = 2Sb^{+++++} + 5PbSO_4 + 10H_2O + 5SO_4^{=}, \quad (V)$$

where the final chemical condition of the oxidized antimony[3] is not known but is immaterial to the result. Thus:

$$\begin{array}{rcl} 21 & x & \\ 2Sb & + 3PbO_2 \rightarrow & 3PbSO_4, \quad x = 62 \text{ g} \\ 2 \times 122 & 3 \times 239 & \end{array}$$

$$\begin{array}{rcl} 21 & x & \\ 2Sb & + 5PbO_2 \rightarrow & 5PbSO_4, \quad x = 103 \text{ g} \\ 2 \times 122 & 5 \times 239 & \end{array}$$

while these results are still short of accounting for the measured self-discharge, they are at least beginning to approach it.

There is yet one other possibility for reduction of PbO_2. An experiment was performed in which PbO_2 was taken from a freshly-formed positive plate, ground up, and placed in a fritted glass filter under 1.300 H_2SO_4. Hydrogen gas from a tank was bubbled up through the PbO_2 layer for one month, and thereafter the solid material was examined by x-ray diffraction. A strong $PbSO_4$ pattern was found to be present in addition to the PbO_2 pattern. Evidently hydrogen gas will reduce PbO_2 under these conditions. The mechanism for this process is not known. It could correspond to direct reduction of PbO_2 to PbO and subsequent reaction of PbO to form $PbSO_4$; or it could come about by oxidation of water to O_2 (i.e., the oxygen overvoltage reaction) where the H_2

[3] The pentavalent state seems likely (8).

would be acting as a depolarizer to speed up the reaction. Either of these reactions is thermodynamically possible, and in the second case a reaction corresponding to equation (II) would occur, except that the oxygen would be converted to water by the depolarizing action. Thus the possibility exists that hydrogen produced by self-discharge at the negative plate may contribute to the reduction of PbO_2 in the positive.

In conclusion it may be said that, although the data do not permit a quantitative interpretation of self-discharge at the positive plate, the available information indicates that it is primarily due to oxidation of the antimony phase in the grid.

Any discussion of this paper will appear in a Discussion Section, to be published in the July 1953 issue of the JOURNAL.

REFERENCES

1. G. W. VINAL, "Storage Batteries," 3rd ed., p. 123, John Wiley & Sons, Inc., New York (1924).
2. A. C. ZACHLIN, *Trans. Electrochem. Soc.*, **82**, 365 (1942).
3. A. C. ZACHLIN, *Trans. Electrochem. Soc.*, **92**, 259 (1947).
4. R. H. GREENBURG AND B. P. CALDWELL, *Trans. Electrochem. Soc.*, **80**, 71 (1941).
5. G. W. VINAL, "Storage Batteries." 3rd ed., p. 129, John Wiley & Sons, Inc., New York (1924).
6. J. J. LANDER, *J. Electrochem. Soc.*, **98**, 213 (1951).
7. J. J. LANDER, *J. Electrochem. Soc.*, **98**, 220 (1951).
8. W. M. LATIMER, "Oxidation Potentials," p. 109, Prentice-Hall, Inc., New York (1938).

An Electrochemical Evaluation of Manganese Dioxide for Dry Battery Use[1]

N. C. Cahoon

National Carbon Research Laboratories, Cleveland, Ohio

ABSTRACT

The factors governing the electrochemical behavior of manganese dioxide in dry cells have never been adequately correlated with the usual physical and chemical properties of this material. Two tests are described, (*a*) determination of the *p*H-potential relation in zinc and ammonium chloride electrolyte and (*b*) determination of the "utilization factor," i.e., the extent of cathodic reduction in a continuous stream of fresh electrolyte. In combination, these give valuable information regarding the general suitability of a sample for dry cell use and afford a partial measure of intrinsic depolarizer capacity, heretofore not obtainable by other than actual battery tests.

Introduction

Throughout the development of the dry cell industry it is doubtful that any single problem has claimed as much technical attention as the selection of manganese dioxide for depolarizer preparation. As early as 1868, Leclanché himself drew attention to the need for proper choice of this important ingredient.[2] Although the subsequent advance in dry cell technology has established the importance of certain depolarizer properties such as high MnO_2 and low impurity contents, it has long been recognized that chemical analyses alone are insufficient to evaluate any particular sample of MnO_2 for battery use. In recent years physical testing methods (2, 3), e.g., x-ray diffraction and electron microscope examination, have been studied as possible evaluation methods and their use has considerably extended our knowledge of the crystal structure of MnO_2. In spite of these advances, no satisfactory laboratory method of evaluating depolarizers has been made available and actual trials in operating cells have been necessary to establish their battery quality. Such tests are both time-consuming and expensive and integrate so many factors (4) that the intrinsic quality of the depolarizer itself may be overshadowed.

This paper presents two tests: the first, a quick evaluation method, based on the relationship between the potential of MnO_2 and the electrolyte *p*H, previously described (5), applicable to battery grade manganese ores and to some extent to synthetic MnO_2; the second, a "utilization test" offering a direct quantitative measurement of depolarizer capacity. Both tests are electrochemical and, therefore, better adapted to give results dependent on the battery properties of a depolarizer than the indirect chemical or physical tests often suggested (6, 7).

General Discussion

pH-Potential Relationship

Extension of previous work (5) has shown that manganese ores from sources other than the African Gold Coast may deviate materially from the straight line *p*H-potential function previously established. Fig. 1 shows a comparison of the data obtained from Java, Caucasian, and Montana samples with that of African ore. The shape and position of the *p*H-potential curve not only furnishes an indication of the suitability of the material for dry cell use, but, in addition, may suggest the type of service application to which a particular depolarizer sample is best adapted.

Interpretation

This correlation depends on the fact that the development of *p*H in the cathode mix of a dry cell depends on the type of discharge to which the cell is subjected. Under heavy drain conditions, such as 4-ohm continuous test on a "D" size (8) cell, nominally 1¼ in. in diameter and 2¼ in. in length, the author has shown (4) that the cathode *p*H is in the 8–10 range for a considerable part of the cell life. Table I compares the potentials of African, Montana, and Java[3] ores at *p*H 9, shown in Fig. 1, with the service of "D" size cells made with the same ores on the 4-ohm continuous test.

Here the order of the potentials developed by the

[1] Manuscript received June 28, 1951. This paper prepared for delivery before the Buffalo Meeting, October 11 to 13, 1950.

[2] "... le meilleur est celui qui est connu dans le commerce sous le nom de manganèse aiguillé: il est cristallisé, soyeux, et possède un éclat graphitoide très prononcé; s'il joint à ces différents caractères une certaine dureté, il possedéra le pouvoir conducteur le plus considerable" (1).

[3] We have found that samples of Java and Caucasian ores possess similar potential-*p*H relationship and generally provide the same order of cell service; they are therefore classified together.

three ores from highest to lowest is African, Montana, and Java which corresponds exactly to the order of the service[4] obtained from these ores in actual cells.

On very light drain tests, such as those characteristic of telephone cells, the cathode *p*H is maintained in the range 5.5–6.0. As shown in Fig. 1, the potential-*p*H curves cross one another in the *p*H range 4.5 to 6.0 and until more is known about the factors responsible for this change in position it seems hazardous to place much emphasis on the relative potential values in this *p*H range. However, below *p*H

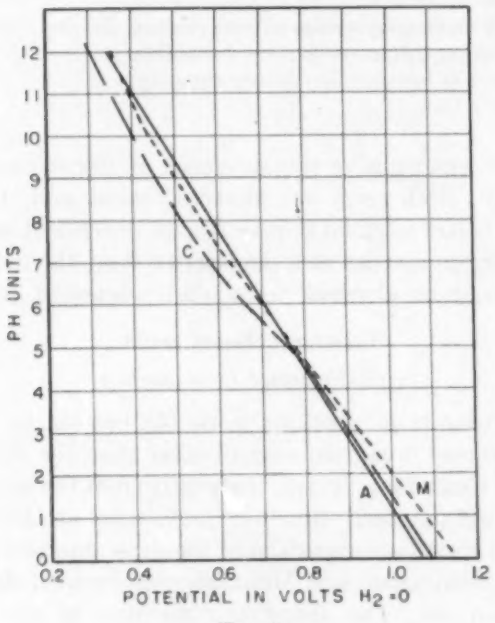

FIG. 1

TABLE I

Depolarizer ore source	Africa	Montana	Java
Minutes service on 4-ohm continuous test on a "D" size cell	539	465	359
Depolarizer potential at *p*H 9	0.52	0.50	0.46

4.5 the relative positions of the three curves are well established. Table II compares the potentials of African, Montana, and Java ores at *p*H 4, shown in Fig. 1, to the 20-ohm light intermittent (telephone) service of No. 6 cells.

It is clear that the order of the potentials developed by the three ores from highest to lowest is Montana, Java, and African, which corresponds exactly to the order of service obtained from these ores in actual cells. Although we recognize that the use of potential values in the *p*H range below 4.5 to indicate performance of cells with a cathode *p*H range 5.5–6.0 is not free from objection, it should be noted that this test has been used successfully in our own laboratories for over ten years without encountering serious discrepancies.

With the curves of Fig. 1 for reference, the potential-*p*H curve of an untried MnO_2 sample furnishes a basis on which the quality of the new material may be judged. Thus, if the potentials of the untried sample are close to or higher than those of the established ores at the same *p*H values, the sample is worth further testing. Although similarity of curve

TABLE II

Depolarizer ore source	Montana	Java	Africa
Days service on 20-ohm light intermittent test on a No. 6 cell	440	425	370
Depolarizer potential at *p*H 4	0.86	0.84	0.83

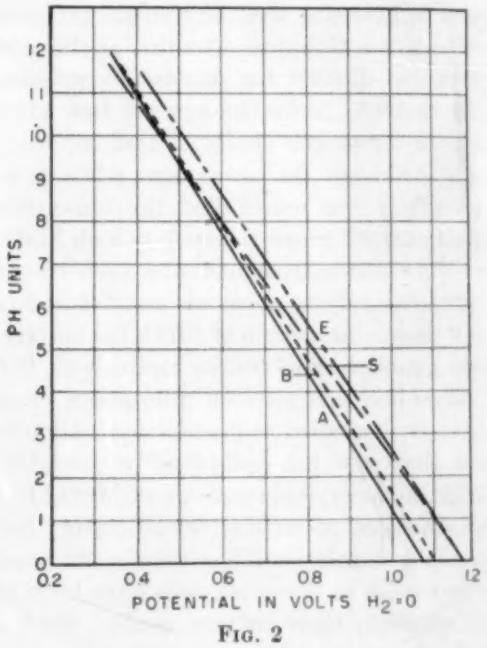

FIG. 2

location and shape provides no absolute assurance that service levels equivalent to those of the established depolarizer will be obtained, close similarity does suggest that, if no interfering factors are present, similar service performance should develop. If, on the other hand, the potentials of the untried sample are definitely lower than those of the established ores, the sample should be regarded as of questionable value and further testing is unnecessary.

Fig. 2 shows the application of the *p*H-potential evaluation method to beneficiated and synthetic MnO_2 samples. Curve E represents an electrolytic MnO_2, curve S a synthetic precipitated type imported from Germany before World War II, curve B

[4] The data presented herewith were obtained during a comparison of ores made several years ago and the service levels are therefore somewhat lower than those of present-day product.

a beneficiated[5] natural ore, and curve A the African ore, previously shown in Fig. 1. All show a straight line *p*H-potential relationship with a slope approximating 0.06 similar to that of the natural African ore, and their higher potential levels through the useful *p*H range indicates that these materials may be excellent depolarizers. The fact that both the electrolytic and imported synthetic MnO_2 have been used successfully for many years in commercial dry cell production has adequately established them as high quality depolarizers. The beneficiated ore, as suggested by the position of curve B has been found to possess a depolarizer value for many applications intermediate between that of the truly synthetic samples and the natural ore.

McMurdie, Craig, and Vinal (9) obtained *p*H-potential relationships with slopes of 0.12 and 0.06 for MnO_2 in the *p*H ranges 2–6 and 6–12, respectively. Previously published data (5) suggest that the discrepancy in the lower *p*H range may be explained by their use of solutions containing hydrochloric acid instead of the zinc and ammonium chloride electrolytes employed in our own work.

Method

The method used for determining the potential-*p*H relationship of a sample of manganese ore closely follows that previously described (5). Electrodes containing the MnO_2 sample under investigation are exposed to a series of eight or ten electrolytes ranging in *p*H from 1 to 12[6] and the potentials developed are determined. The preparation of the electrodes and the general test procedure are as follows.

A mixture of three parts by weight of manganese ore and one part by weight of battery grade Acheson graphite such as No. 697 is milled to approximately 200-mesh fineness. A portion of this mixture is spread in a layer about 1/16 in. (0.16 cm) thick on a dry rectangular strip of muslin 1/2 in. (1.27 cm) by 3/4 in. (1.90 cm). The strip is then wrapped around one end of a wax-impregnated carbon electrode 0.161 in. (0.41 cm) in diameter by 1.88 in. (4.77 cm) long, the powdered material next the carbon, and held in place by three tightly stretched rubber bands. Three such electrodes are mounted on a thin perforated rubber stopper by forcing the uncovered ends of the carbon electrodes through tightly fitting holes so that the carbon rods protrude a short distance to permit electrical contact. The assembly of three electrodes is inserted into a sample jar containing sufficient electrolyte to immerse completely the MnO_2-carbon layer. An additional hole in the stopper permits the insertion of a saturated type calomel reference electrode side neck or salt bridge. After two to three days of contact with the electrolyte, the electrodes have reached equilibrium and potential readings are then made. Immediately following the potential readings the stopper and electrode assembly are removed for the *p*H determination on the electrolyte sample used. By application of the proper factor for the temperature of the electrolytes at the time of the measurement the potential values may be expressed with reference to the normal hydrogen electrode.

The test described establishes a basis on which MnO_2 samples may be readily differentiated into those worth further examination and those which need no further consideration. In spite of the success with this rapid test method we early recognized that additional measurements, particularly of the depolarizing capacity, would greatly extend the scope and value of any laboratory testing program for depolarizers. The results of our efforts to develop a means of determining depolarizing capacity culminated in the "utilization test" described below.

The Utilization Test

To integrate the factors controlling battery quality, an electrochemical method for direct determination of the depolarizing capacity of a sample of MnO_2 offers obvious advantages. Such a test should meet several requirements, among them:

1. It should involve a measurement of the intrinsic depolarizing capacity of the sample, in which extraneous factors such as variation in electrolyte composition and *p*H and the precipitation of by-products during the test would be eliminated.

2. The potential or other readings on the MnO_2 should be independent of any variation in the other cell electrode, i.e., they should be made against some reference electrode external to the test unit.

3. Readings should be made in such a manner that the *IR* drop due to current passing through the cell is not a factor.

4. To make the test generally applicable it should give reproducible results and require a relatively short time-period for completion.

About 30 years ago, French and MacKenzie (11) reported that, if dry battery electrolyte were circulated through a manganese dioxide cathode, the manganese, instead of being converted to the trivalent state as in the dry cell, was reduced to the divalent state and appeared in the effluent as manganous chloride. The reaction at the cathode[7] may

[5] The beneficiated ore was prepared by acid leaching Mn_2O_3, prepared from African ore, to form MnO_2 and a manganese salt. The MnO_2 was washed free of residual acid and salt and then dried. Patents by Burgess (10) and others cover variations of this process.

[6] Compositions yielding convenient *p*H values are given in the earlier paper (5).

[7] This reaction has also been postulated by McMurdie, Craig, and Vinal (9) for electrolytes containing hydrochloric acid.

be represented thus:

$$2e + MnO_2 + 4H^+ \rightarrow Mn^{++} + 2H_2O. \quad (I)$$

This technique offered a basis for a method which would meet the requirements presented above.

In view of all the attractive features presented by a cell with flowing electrolyte, a laboratory test unit was designed in which accurately measured amounts of MnO_2 could be discharged cathodically under these conditions. A current density of 6.5 amp/ft^2 (0.007 amp/cm^2) (which is approximately that at the zinc anode in a size "D" cell on 4-ohm test) was chosen and arrangements provided to maintain it at a constant value throughout the test. The polarized open-circuit potential[5] of the MnO_2 electrode, followed as the discharge proceeded, indicated the progress of the test. The test was considered complete when the potential had fallen to the value of 0.26 volt positive to a saturated calomel reference electrode, this cutoff being selected as the mean of values found in actual "D" size cells discharged on a 4-ohm test, e.g., the Industrial Flashlight Tests

TABLE III

Sample	Utilization factor (%)
African ore	40
Electrolytic MnO_2	70–76
Imported chemical MnO_2	78
Beneficiated African MnO_2	50

(8) at the 0.9 volt cutoff. The service, in minutes, obtained to this cutoff potential, expressed as a percentage of that equivalent to all the MnO_2 present in the test sample, was designated the "utilization factor."

Interpretation

A group of representative depolarizers tested as described gave the results shown in Table III.

The wide range of values shown in Table III suggests that this test provides a measure of some factor characteristic of the individual material examined. This variation is not due to a lack of reproducibility for three tests on the same sample of depolarizer gave values of 62.0, 63.6, 65.2 per cent with an average of 63.6 per cent and an average deviation of only 1.1 per cent. During the test, MnO_2 is reduced to $MnCl_2$, i.e., $Mn^{IV} \rightarrow Mn^{II}$.* This, of course, means a valence change of 2, which, since the electrolyte *p*H was 3.85, would be in accordance with the 0.12 slope of the *p*H-potential relationship descriped by McMurdie, *et al.* (9), rather than with the 0.06 value of Fig. 1 and 2. The factors responsible for this apparent discrepancy have not been identified.

The reduction to the divalent stage represents twice the output of electrical energy per unit of MnO_2 obtained when MnO_2 is reduced to $Mn_2O_3 \cdot H_2O$ or $ZnO \cdot Mn_2O_3$, i.e., $Mn^{IV} \rightarrow Mn^{III}$. However, as shown in Fig. 3, the MnO_2 potential curve obtained in the course of this test is strikingly similar in shape to the normal dry cell discharge curve. Curve B was obtained from experiments using an African ore sample which gave about 100 minutes service on "utilization test," equivalent to a utilization factor of 42 per cent. Curve A shows the normal

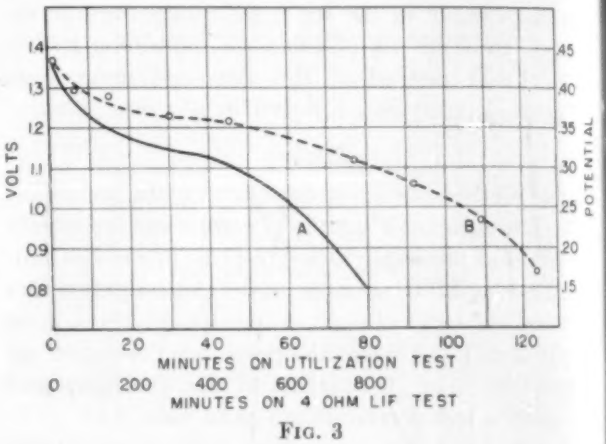

FIG. 3

discharge curve of an African ore "D" size flashlight cell on 4-ohm light Industrial Flashlight Test.

Obviously the utilization test as shown cannot integrate all of the factors operative during dry cell discharge. It does not identify the type of end product or the amount that would form under battery discharge conditions. However, the test does measure some properties of a depolarizer which are closely related to its operation and this brings us one step closer to the better understanding of the depolarizer reaction mechanism. As in the case of the pH-potential test, the utilization test offers an excellent means of differentiating depolarizers: those which meet or surpass the levels given in Table III are definitely worth further examination and evaluation in cells, whereas those which fail to do so require no further consideration.

In addition to its value as a testing mechanism, the utilization test offers a possible explanation of some phases of dry cell depolarization. It seems clear that the electrochemical cathodic reaction in the dry cell may well be that given earlier in this manu-

[5] Open-circuit potential measurements, made during a momentary breaking of the circuit, probably included considerable polarization and so were not obtained under true equilibrium conditions.

* In a representative test lasting 102 min, the electroreduction of Mn^{IV} to Mn^{II} would have accounted for 0.1883 g of manganese (as chloride) in the effluent solution. The amount of Mn^{II} determined by actual analysis was 0.1897 g.

script as equation (I), mainly a reduction of Mn^{IV} to Mn^{II}. Secondary chemical reactions presumably of the type

$$MnO_2 + Mn^{++} + 2H_2O \rightarrow Mn_2O_3 \cdot H_2O + 2H^+ \quad (II)$$

suggest the mechanism for the disposal of Mn^{II} produced electrochemically to form the well-known end product $Mn_2O_3 \cdot H_2O$. This suggestion is in agreement with the data of McMurdie, *et al.* (9), based on their equilibrium studies. True equilibrium conditions may not often occur in an operating dry cell cathode due to the important part played by diffusion of anodically produced zinc chloride in influencing the cathode *p*H. Under these conditions the reaction steps suggested herewith offer at least a first approximation to the mechanism involved in the dry cell cathode operation.

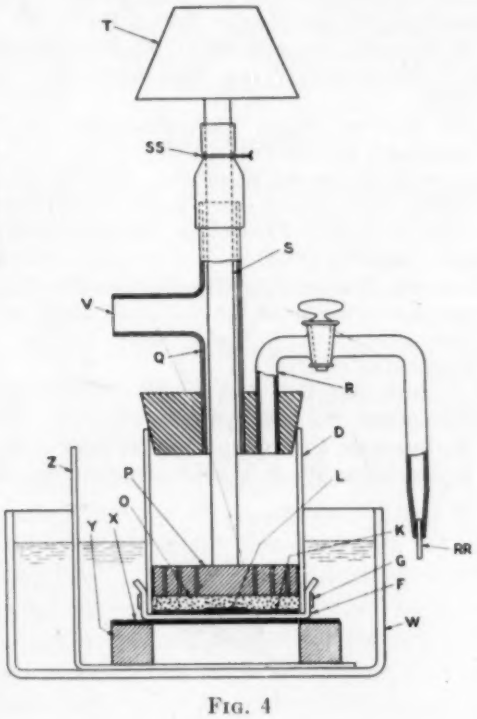

FIG. 4

Method

The electrolytic cell developed for the utilization tests is shown in Fig. 4. A cathode layer of MnO_2, acetylene black mix, and its overlying coating of coke is mechanically compressed between a perforated graphite contact disk and a cellulose diaphragm by means of a weight acting on the top of the graphite disk. A "Nichrome" screen supports the diaphragm, and arrangements are provided for forcing electrolyte through the cathode continuously during the test. A hard rubber ring, Y, ½ in. (1.27 cm) high, $1\frac{13}{16}$ in. (4.60 cm) inside diameter and $2\frac{13}{16}$ in. (7.13 cm) outside diameter supports the "Nichrome" screen, X, and insures a fixed distance between the cathode and the zinc anode, Z.

The cathode chamber, D, consists of a $2\frac{5}{16}$ in. (5.87 cm) length of plastic tubing, e.g., "Lucite," $1\frac{13}{16}$ in. (4.60 cm) inside diameter and $\frac{1}{16}$–$\frac{1}{8}$ in. (0.16–0.32 cm) wall thickness. One end of this tube is closed with a diaphragm, F, comprised of a ten-ply layer of absorbent cellulosic paper, commercially available as cleansing tissue, and one external layer of thin cotton fabric applied so that it is free from wrinkles and is held in place by tightly stretched rubber bands, G. A portion of the MnO_2 sample containing 0.7100 gram MnO_2, which has been ground in a mortar for three minutes with 0.113 gram acetylene black, is distributed on the inside of the diaphragm in a uniform layer, K, covering the whole area, with the exception of a space at the center which is occupied by a hard rubber disk, L, ½ in. (1.27 cm) in diameter and $\frac{1}{16}$ in. (0.16 cm) thick. A 5-gram quantity of battery grade coke, O, is uniformly distributed over the layer of mix and the hard rubber disk and is pressed down firmly with a flat-ended rod loosely fitting the plastic tube. The perforated graphite disk, P, to be placed on top of the coke layer, is $\frac{3}{8}$ in. (0.95 cm) thick, fits the inside of the plastic tube loosely and, except for a ½ in. (1.27 cm) diameter portion at the center, has 95 equally spaced 0.045 in. (0.114 cm) holes drilled completely through it.

The upper end of the plastic tube is fitted with a two-hole rubber stopper carrying a glass tee, Q, located at the center and an additional tube, R, provided with a stopcock and an outlet tube bent as shown in Fig. 4. Through the center of the glass tee is placed a $\frac{5}{16}$ in. (0.79 cm) diameter carbon rod, S, which provides contact with the perforated graphite disk in the cell at the lower end and transmits the mechanical pressure provided by the 3 kg weight, T. The side neck, V, of the tee, Q, furnishes a connection for the electrolyte supply which can be arranged in any convenient manner. The tube, R, containing the stopcock, is provided to permit a liquid path from the back of the cathode to the saturated calomel-type half cell and may be fitted with a paper plug at RR as shown.

To perform a test, the apparatus is assembled, the cell chamber, calomel cell connecting tube and crystallizing dish, W, are filled with electrolyte and the rubber tubing at the top of the glass tee tightly clamped around the carbon pressure rod with a twisted wire, SS, to prevent electrolyte leakage at this point. The electrolyte supply is then adjusted to maintain a continuous flow of 2.0 ± 0.2 ml per minute. The electrolyte used in the work described contains 33 per cent $ZnCl_2$, 20 per cent NH_4Cl, and 47 per cent water and possesses a *p*H of 3.85. The

cell is discharged on a constant current of 0.108 amp, connections to the external circuit being made at the exposed parts of the zinc anode, Z, and rod, S. Periodic measurements of the open-circuit potential of the cathode, the electrical connections being taken from rod S and a calomel cell through a salt bridge contacting RR, are made with a potentiometer and a galvanometer such as a Leeds and Northrup 2500-B reflecting type with appropriate lamp and scale. The measurement of the polarized open-circuit potential of the cathode is made as rapidly as possible while a switch in the discharging circuit is opened momentarily. The test is considered complete when this polarized open-circuit potential value falls to 0.26 volt positive to the saturated type calomel cell. The 0.7100 gram quantity of MnO_2 has a theoretical service capacity of 244 minutes at 0.108 amp. The utilization factor can be readily calculated by expressing the amount of service to the cutoff as a percentage of this value.

Conclusions

Two methods suitable for the laboratory examination of dry cell depolarizers are described in the present paper. The first is a rapid evaluation based on the relationship between MnO_2 potential and electrolyte *p*H described in a previous publication (5). The second is based on a direct electrochemical measurement of depolarizer capacity under cell discharge conditions. Although neither of these tests alone is definitive, their combination affords a good insight into the probable behavior of a sample of MnO_2 under battery conditions. Any materials that prove substandard on these two tests can be eliminated from further consideration and only those that meet the test requirements need be subjected to final battery evaluation.

Acknowledgment

The author wishes to express his thanks to Mr. G. W. Heise for his contributions to this work, which was conducted under his direction.

Any discussion of this paper will appear in a Discussion Section, to be published in the July 1953 issue of the Journal.

References

1. G. Leclanché, "Pile au peroxyde de manganèse à un seul liquide," *Les Mondes* (Paris), **16**, 532–535 (1868).
2. P. H. Delano, *Ind. Eng. Chem.*, **42**, 523 (1950).
3. H. F. McMurdie, *Trans. Electrochem. Soc.*, **86**, 313 (1944).
4. N. C. Cahoon, *Trans. Electrochem. Soc.*, **92**, 159–172 (especially pp. 168–169) (1947).
5. N. C. Cahoon, *Trans. Electrochem. Soc.*, **68**, 177 (1935).
6. O. D'Agostino, *Ricerca sci.*, **9**, No. I, 195 (1938).
7. C. Drotschmann, *Chem. Ztg.*, **56**, 234 (1932), from *C. A.*, **26**, 3734 (1932).
8. "American Standard Specification for Dry Cells and Batteries, Circular of the National Bureau of Standards, C435," U. S. Government Printing Office, Washington (1942).
9. H. F. McMurdie, D. N. Craig, and G. W. Vinal, *Trans. Electrochem. Soc.*, **90**, 509 (1946).
10. C. F. Burgess, U. S. Pat. 1,305,250, June 3, 1919.
11. H. F. French and A. A. MacKenzie, unpublished work.

The Electrodeposition of Silver on an Iron-Nickel Alloy for a Glass-to-Metal Seal Arrangement[1]

R. T. Foley

TAP Laboratory, General Electric Company, Pittsfield, Massachusetts

AND

R. D. Alvord and J. K. Easley

High Voltage Bushing Engineering, General Electric Company, Pittsfield, Massachusetts

ABSTRACT

A method of silver plating a 58 per cent iron-42 per cent nickel alloy to produce an electrodeposit capable of withstanding an anneal at 850°C is given. The surface preparation of the alloy, the proper salt concentration of the "strike" bath, and the plating step are described. No nickel or copper undercoating is used to achieve an adherent coating. The diffusion of oxygen through this silver plate is hindered by a thin coating of indium which also sponsors the glass-to-metal seal.

Introduction

This investigation is concerned with electroplating a 58 per cent iron-42 per cent nickel alloy with silver so that the material will have certain high temperature properties and be compatible in a glass-to-metal seal arrangement.

The manufacture of cast glass bushings for electrical apparatus has been outlined by Easley (1). A lead-free borosilicate glass in the molten state is poured into a mold holding an iron-nickel alloy flange. After cooling slightly, the cast structure is moved to a furnace at about 550°C, annealed for several hours, and finally removed from the furnace at about 100°C. Although it is acknowledged that iron-nickel alloys possess considerable resistance to high temperature oxidation, scaling does occur during this process. The oxide scale must be removed before the flange may be soldered during the assembly of the apparatus. Thus it is of engineering importance to protect this alloy from oxidation during the processing. One means of accomplishing this is to electrodeposit silver over the iron-nickel alloy.

The major problems which were posed had to do with the proper surface treatment of the iron-nickel alloy to attain an adherent plate, the reluctance of silver to be wet by molten glass, and the high rate of diffusion of oxygen through silver plate. While considerable effort has been expended in the development of methods of silver plating ordinary steel, it was questionable at the start how much of this knowledge would be applicable to the electrodeposition of silver on this iron-nickel alloy.

[1] Manuscript received December 19, 1951. This paper prepared for delivery before the Detroit Meeting, October 9 to 12, 1951.

Experimental

Materials and Equipment

The alloy[2] used in this investigation had a composition of 58 per cent iron and 42 per cent nickel with a maximum carbon content of 0.15 per cent. Its thermal expansion curve matches quite closely the expansion curve of a lead-free borosilicate glass used in the manufacture of cast glass bushings. As a preliminary step this alloy is annealed at 1125°C in an hydrogen atmosphere (dew point approximately −50°F), a treatment which is effective in degassing and decarburizing the metal (methane reaction) so that no bubbling takes place when the glass is cast.

The first experiments in developing the plating method were carried out with solutions of one liter volume. Larger baths, 17 liters in volume, and finally factory size baths up to 750 liters, were employed as the development progressed.

The Plating Process

The entire treatment of the iron-nickel alloy may be broken down into several separate steps. From the study of the literature and as the development went forward it was evident that simply silver plating was not sufficient to produce an electroplate of the properties required for this particular engineering application. In order to develop a surface which would participate in the glass-to-metal seal and be resistant to the diffusion of oxygen, it was necessary to cover the silver plate with a thin coating of indium. Thus the entire process included the following steps: surface preparation of the alloy; silver "striking"; silver plating; and indium plating. The

[2] Furnished by the Carpenter Steel Company, Reading, Pa.

detailed discussion of such conventional operations as degreasing and rinsing is purposely omitted. Before the initial pickling, the samples were vapor-degreased in trichlorethylene and between the successive operations, with the exception of the "striking" step and the "plating" step, the parts were rinsed in warm water.

Surface Preparation of the Alloy

The proper method of cleaning the iron-nickel alloy is dictated in part by its previous treatment. In the authors' process, part of this treatment included the hydrogen firing at 1125°C, and although the parts came to the plating step relatively free of organic matter, they were coated with an oxide layer which was difficult to remove by conventional methods.

This oxide layer is very obvious if, following the hydrogen firing at 1125°C, the parts are not cooled almost to room temperature. Even when the parts are allowed to cool to room temperature in an hydrogen atmosphere and are then allowed to stand exposed to normal atmospheres, an oxide layer sufficiently thick to interfere with electroplating develops. Electron diffraction examination (2) of the first-formed oxide film on the surface yielded only the pattern for nickel oxide. Thicker films gave more complex patterns, including the lines for Fe_2O_3, and possibly mixed crystals of the oxides of nickel and iron. Many conventional methods of cleaning were examined before two were chosen as suitable to give a surface satisfactory to electroplate. Surface preparation by an anodic acid pickle was not examined exhaustively although it was noted that anodic cleaning of ordinary steel in HCl or H_2SO_4 followed by striking with Ni, Cu, or Ag was detrimental to the bond between the steel and the electroplate (3).

The first method involves pickling the alloy in an acid mixture at elevated temperature. The acid mixture is composed of 1 part by volume of concentrated HCl (37%), 1 part of concentrated H_2SO_4 (96%), 1 part of concentrated HNO_3 (70%), and 9 parts of H_2O. The time required to achieve a visually clean surface varies with the temperature of the bath, being of the order of 5 minutes at 60°–65°C and 30 seconds at 90°–95°C. The higher temperature is recommended because the loss in metal is of the order of 1–2 per cent as compared with 10 per cent at the lower temperature and longer time. (This percentage applies only to the parts here under consideration.) After this pickling operation a black residue remains on the surface. This is removed by dipping in a solution composed of 2 parts of concentrated H_2SO_4 and 1 part of HNO_3 for 15–20 seconds. After rinsing, the part is transferred to a solution of KCN (50 g/l) to neutralize any residual acid.

A second method involves the cathodic treatment of the alloy at room temperature in the above pickling solution or in a 10 per cent solution of H_2SO_4. A cathode current density of about 2.6 amp/dm² is used for 15 minutes. During the early experiments stainless steel (18/8 Cr/Ni) anodes were employed. Their undesirable and costly dissolution, as well as the resultant contamination of the bath, led to their replacement with carbon anodes. It was felt that a common deterrent in the use of carbon anodes, namely, separation and electrophoretic migration of carbon particles, would not interfere because of the bright-dipping step which followed the acid pickling. This was borne out experimentally.

In a continuous factory operation the use of the mixture of acids at elevated temperature would certainly pose problems of equipment maintenance. Thus the second method is used in preference to the first.

It has been suggested that the highly etched surface would lend itself to the development of a more adherent plate by virtue of a "mechanical keying" effect (4). This theory was appraised experimentally and the conclusion was reached that the roughness of the steel contributed only in a minor way to the adherence of plate (5).

The Silver "Striking" Step

It is generally accepted that steel may not be plated without a "strike" and preliminary experiments using techniques suggested in the literature to plate directly on steel were not successful in achieving a plate which would not blister when the part was annealed in H_2 at 850°C.

The composition of a "strike" bath which is believed to be of the proper composition contains 1.0 g/l of silver cyanide and 80 g/l of potassium cyanide. A series of experiments established that the silver cyanide content must not exceed 3.75 g/l if an adherent plate (after annealing) is to be obtained. Stainless steel (18/8) anodes are used in this bath.

A necessary requirement is that the alloy part be carried from the neutralizing step to the "striking" bath without drying and immersed in the strike bath with the current on. A part is treated cathodically with a current density of 1.7 amp/dm² until it is covered completely with a shiny plate of silver. This current density may be varied between 1.0–2.6 amp/dm² without adversely affecting the quality of the plate. The "strike" usually requires 30 seconds to one minute. In some cases the part is allowed to plate in the "strike" bath for several minutes after the first coating is applied to render less likely exposing the alloy during transfer to the plating bath.

The Silver Plating Step

With the exception of the speed at which the plate is applied to the iron-nickel alloy, the plating

procedure is quite conventional. The solution composition is: silver cyanide, 30 g/l; potassium cyanide, 42 g/l; potassium carbonate, 45 g/l.

The current density is 0.4 amp/dm² at room temperature. Silver anodes (99.9% silver) are employed. It was established that at least at the start of the plating process a low current density is desirable. During early experiments a current density of 0.2 amp/dm², which was increased to 0.85 amp/dm² after 15 minutes (total plating time 45 minutes), was employed. This was later changed to the single rate of 0.4 amp/dm² to allow parts to be placed in and withdrawn from the single bath with only current change to account for the area being plated. Thicknesses of silver up to 0.063 mm were plated by this method and found to be adherent by the 850°C H_2 annealing test. The bath concentration is maintained by the usual periodic analyses.

After silver plating, the parts are tested by firing in hydrogen for 15 minutes at 850°C.

Test for Adherence

The required degree of adherence between an electrodeposited coating and its basis metal is often decided by the particular engineering application involved. This was true in the development undertaken by the authors where the conditions imposed on the electroplated alloy by future manufacturing operations dictated what adherence was necessary. Some mechanical strength and the ability to withstand a thermal shock without blistering was required. During the manufacturing process molten glass at 900°–1000°C is poured over the metal part in a mold at about 500°C.

It was found that a fair test for adherence was simply to place the plated alloy directly in an hydrogen atmosphere at 850°C and hold it at this temperature for 15 minutes. Parts that passed this test, i.e., did not blister, went satisfactorily through the manufacturing process which included the casting operation and the air anneal. It should be pointed out that this hydrogen anneal is not necessary to get "adherent" plates. Iron-nickel parts may be plated, cast into bushings, and annealed without blistering. Moreover, there was no indication that poor plates could be repaired by hydrogen firing. In order to study the adherence developed by a particular plating process many cross sections were examined microscopically. No tendency for silver to alloy with the basis metal was observed in these sections (Fig. 4).

While this annealing is not necessary to get good adhesion, there is evidence in the literature from a study of a similar treatment of electrodeposited silver on ordinary steel (6) that an extended hydrogen anneal at elevated temperature does improve the adherence.

It was observed that it is relatively easy to get silver plates which are not blistered after plating or after ordinary handling. The thermal shock, however, is a critical test for adherence.

The Indium Plating Step

The silver-plated parts are dipped into a solution of potassium cyanide (50 g/l) before being plated with a thin layer of indium. A current density of 1.7 amp/dm² is employed with the conventional cyanide bath (7). Steel anodes are used and the bath is maintained at room temperature. Usually a coating in the thickness range of 0.0002–0.0005 mm is applied. Although it is standard practice to diffuse the indium plate to develop the indium-silver alloy it was found that for this application a separate diffusion step is not necessary. During normal manufacturing operation the part is at elevated temperature and undoubtedly considerable diffusion takes place. The adherence and the achievement of a good glass-to-metal seal is not sensitive to the thickness of the plate—if the thickness is maintained in the order of these thin or "flash" coatings.

Discussion—Properties of the Plate

The thin coating of indium over the silver electroplate influences directly the glass-to-metal seal and indirectly the silver-to-alloy bond.

With the particular glass-casting operation employed, no glass-to-metal seal of any strength develops when glass is cast directly over silver. When a "flash" coating of indium covers the silver, an hermetically tight seal which is stronger than the glass develops. It is postulated that the mechanism involves the wetting of the indium surface by the molten glass, for at the instant of casting there must exist a liquid-liquid system. Fig. 1 presents the cross section of a nickel-oxide seal, used extensively in glass-to-metal seal practice. Nickel oxide probably functions by virtue of its solubility in glass and there appears to be some penetration of glass into the oxide phase and vice versa. Fig. 2 shows a seal in which the promoting component is indium. There is no evidence of an ozidized zone between silver and the glass and the discontinuity of the two phases is apparent. This photomicrograph, however, does not eliminate the possible existence of an extremely thin indium oxide layer.

The type of bond developed between the silver and the alloy by this plating procedure is illustrated in Fig. 3. The alloy was pickled in hot acid before plating, but, with the exception of a smoother steel surface, a cross section of a cathodically cleaned sample is not much different. When hydrogen-annealed for 3 hours at 850°C there is recrystallization of the silver but no apparent change in the silver-to-alloy bond (Fig. 4). The destructive effect of an air

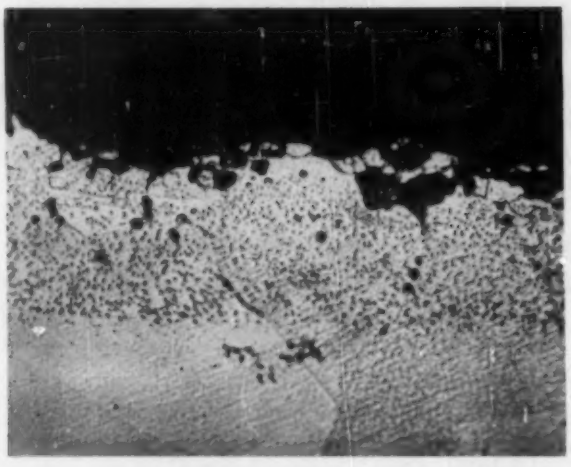

FIG. 1. Cross section of a glass-to-metal seal of the nickel oxide type, showing the nature of the interface between the glass and the iron-nickel alloy. A—glass; B—oxidized interface; C—iron-nickel alloy. Magnification: 600×; etchant: 50 g $FeCl_3$ in 1 l methyl alcohol.

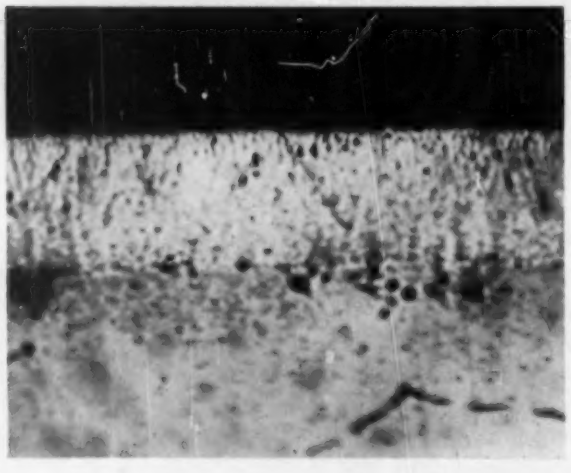

FIG. 2. Cross section of a glass-to-metal seal of the indium type, showing the glass-silver interface. A—glass; B—silver; C—iron-nickel alloy. Magnification: 1000×; etchant: same as Fig. 1.

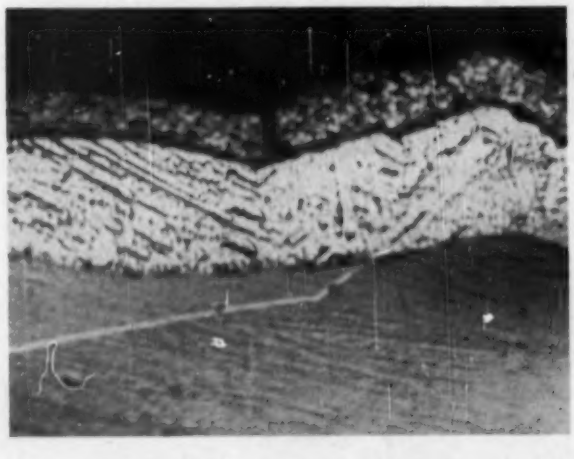

FIG. 3. Silver-plated iron-nickel alloy, as plated, showing silver-alloy interface. A—copper plate (backing); B—silver plate; C—iron-nickel alloy. Magnification: 1000×; etchant: 77 ml of concentrated (28%) ammonia solution + 23 ml of hydrogen peroxide (30%) solution for the silver; same as Fig. 1 for the alloy.

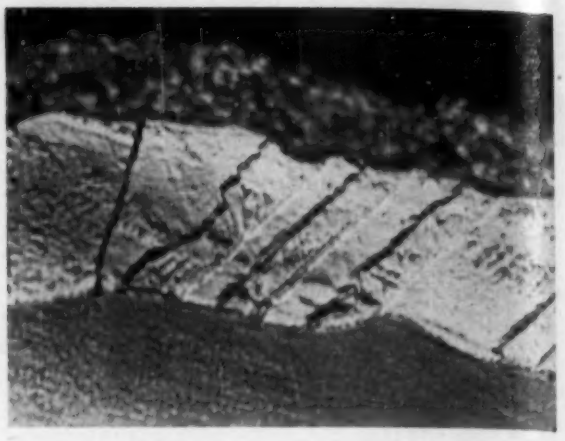

FIG. 4. Silver-plated iron-nickel alloy, annealed in hydrogen atmosphere at 850°C for 3 hr, showing silver-alloy interface. A—copper plate (backing); B—silver plate; C—iron-nickel alloy. Magnification: 1000×; etchant: same as Fig. 3.

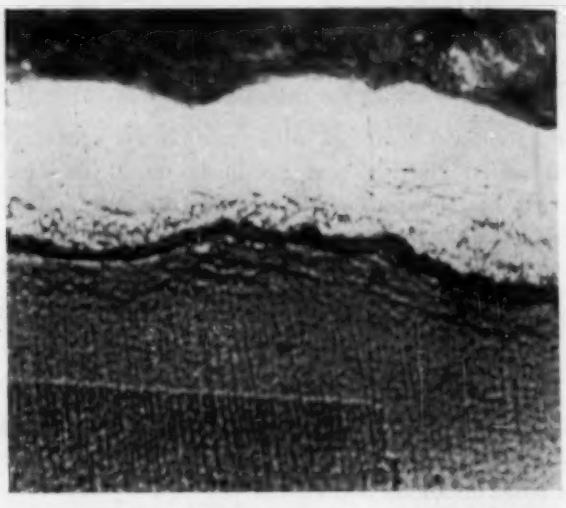

FIG. 5. Silver-plated iron-nickel alloy, annealed in air at 600°C for 4 hr, showing oxidation at silver-alloy interface. A—copper plate (backing); B—silver plate; C—iron-nickel alloy. Magnification: 1000×; etchant: same as Fig. 3.

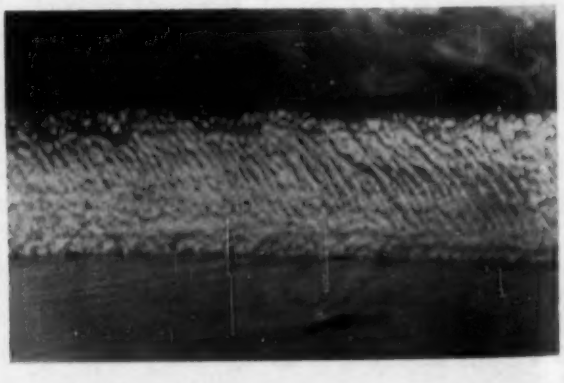

FIG. 6. Silver-plated iron-nickel alloy, indium "flashed" and annealed in air at 600°C for 4 hr, showing that the interface is relatively free of oxidation. A—silver plate; B—iron-nickel alloy. Magnification: 1000×; etchant: same as Fig. 3.

anneal (4 hr at 600°C) with the formation of the oxide scale at the silver-alloy interface is seen in Fig. 5. This effect has been observed before (8). A sample of alloy plated similarly to the last but also given a thin layer of indium was annealed for 4 hours at 600°C. This interface is shown in Fig. 6.

It seems reasonable that at the elevated temperature indium (melting point 155°C) diffuses rapidly into the silver. It has been shown that when oxygen diffuses through a silver alloy it reacts preferentially with that element with which it has the greatest affinity (here indium) to form an internal oxidation zone (9). In silver alloys of high alloy concentration this zone may act as a barrier to further oxygen diffusion. Weight increase-time measurement coupled with microscopic examinations of the interfaces substantiate this proposed mechanism. Data from an air anneal at 700°C given below are representative of severe oxidation, but do give the relative order of magnitude of the two types of reaction.

	Weight increase (mg/cm²)	
	After 1 hr	4 hr
1. Silver plated (0.0076 mm)	0.20	0.69
2. Silver plated (0.0076 mm) with indium flash coating (0.0005 mm)	0.14	0.25

Examination of the samples reveals that in case 1 the oxidation took place entirely at the (silver)-(iron-nickel alloy) interface; in case 2, for the most part, at the surface. There is some evidence of oxygen penetration to the (silver)-(iron-nickel alloy) interface at the longer oxidation times and at raised temperature even with samples treated with an indium "flash" coating.

Acknowledgment

The authors are indebted to Miss M. E. Smith and to F. G. Stone for the metallographic work illustrated in this paper.

Any discussion of this paper will appear in a Discussion Section, to be published in the June 1953 issue of the Journal.

References

1. J. K. Easley, *Elect. Mfg.*, **41**, 112 (1948).
2. H. O. Spauschus, private communication.
3. F. C. Mesle, *Monthly Rev. Am. Electroplaters' Soc.*, **33**, 937 (1946).
4. F. C. Mathers and L. I. Gilbertson, *Trans. Electrochem. Soc.*, **74**, 287 (1938).
5. H. L. Crosby and L. I. Gilbertson, *Trans. Electrochem. Soc.*, **82**, 101 (1942).
6. N. S. Freedman, *Trans. Electrochem. Soc.*, **91**, 325 (1947).
7. J. B. Mohler, *Metal Finishing*, **43**, 60 (1945).
8. J. S. Hart and C. E. Heussner, *Monthly Rev. Am. Electroplaters' Soc.*, **33**, 142 (1946).
9. F. N. Rhines and A. H. Grobe, *Trans. Am. Inst. Mining Met. Engrs.*, **147**, 318 (1942).

Electrolytic Determination of Tin and Tin-Iron Alloy Coating Weights on Tin Plate[1]

C. T. Kunze and A. R. Willey

Exploratory Research Section, Research Division, American Can Company, Maywood, Illinois

ABSTRACT

Tin can be anodically removed from steel in a 1*N* hydrochloric acid solution with full current efficiency. In contrast with electrolytic behavior in alkaline media, the action does not stop at the tin-iron alloy surface but this intermetallic compound is stripped as well. The voltage changes, which develop between a reference electrode and the tin plate specimen (anode), are transmitted to a recording potentiometer which plots a time-potential curve with two end points from which the free and alloyed tin are determined. Apparatus with a specially designed d-c power source is described.

Introduction

The amount of tin, applied as a protective coating on steel, influences the cost of tin plate as a raw material for the container industry, the can manufacturing operations, and the shelf life of the can. In addition, world conditions at the present time necessitate conservation of this strategic metal. For these reasons, the estimation and control of tin coating weights is of considerable importance.

Several methods are now available for determining tin coating weights. Among these are the Sellars (1) and Bendix, (2) which are chemical methods most often used in industrial laboratories. The antimony trichloride-hydrochloric acid procedure (3) is considered by some as the standard or reference method. Francis (4), Hothersall, and Bradshaw (5) have reported electrolytic procedures using sodium hydroxide as electrolyte and recently Beeghly (6) has described an x-ray absorption method.

All of the above methods, except those employing electrolysis, measure the total amount of tin including that which has alloyed with the steel, and as yet no entirely satisfactory procedure for the determination of this alloyed constituent has been described in the literature.

Hot-dipped and also flow-brightened electrodeposited coatings on commercial tin plate have a certain amount of tin alloyed with iron. The thickness of this alloy layer is of considerable importance since it influences container manufacturing operations and also the performance of the can from packer to consumer. It has been demonstrated that the internal corrosion resistance of the container is in part a direct function of the free tin on the surface of the steel and that the alloy affords very little electrochemical protection.

The extent of alloying during hot tinning is usually in the range of 0.15–0.20 lb tin/BB.[2] Adequate free tin is generally present in hot-dipped coatings to allow for normal usage, and the amount of tin converted to alloy has never been considered a problem. In the manufacture of thin electrodeposited coatings the various flow-brightening practices can produce alloys ranging from 0.03–0.18 lb tin/BB. The latter figure in the case of No. 25[3] coatings represents approximately 70 per cent of the total tin with only 0.07 lb/BB of free tin remaining. Sufficient evidence is available to indicate that proper control of the flow-brightening operation can result in the maintenance of alloyed tin within the range 0.03–0.06 lb/BB. The development of a convenient and accurate analytical procedure for the estimation of free and combined tin was a necessary step toward this end.

In addition to the iron-tin compound formed during tin plate manufacture, subsequent organic coating baking operations on the part of the can manufacturer may substantially increase the alloy thickness even though the temperatures employed are below the melting point of tin. Typical alloy growth curves in this temperature range are shown in Fig. 1.

Most of the reactions used to strip the free tin prior to alloy determination either give incomplete stripping, attack the alloy, or a portion of the alloy is lost when the reaction residues are wiped off. Sodium plumbite, sodium hydroxide-hydrogen peroxide, and sodium iodate solutions, all recommended at various times, attack the alloy. The use of silver nitrate to remove the free tin results in a

[1] Manuscript received November 12, 1951. This paper prepared for delivery before the Detroit Meeting, October 9 to 12, 1951.

[2] Base Box as defined by the AISI Steel Products Manual, Tin Mill Products, Section 14, is the estimative unit of area, 112 sheets of tin plate 14 in. × 20 in. or 31,360 in.^{2} (217.78 ft^2).

[3] No. 25 AISI designation for electrolytic tin plate with a nominal tin coating of 0.25 lb/BB. No. 50 has a nominal coating of 0.50 lb/BB.

spongy silver matte remaining on the plate, and as much as 50 per cent of the alloy is wiped off when the silver is removed. Of the methods described in the literature only the electrolytic procedures (4, 5) give satisfactory end points with no appreciable effect on the alloy. However, under the conditions stated, difficulty is encountered in dealing with samples as large as 4 in.² (the standard disk for tin coating determinations) since detinning is incomplete unless the current is reversed several times and often the last traces of free tin can be removed only by immersion in hot (90°C) 10 per cent caustic solution.

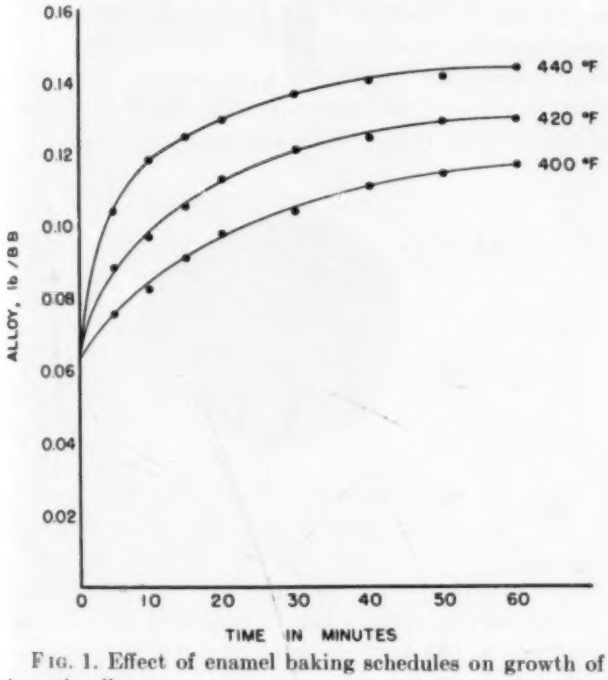

FIG. 1. Effect of enamel baking schedules on growth of iron-tin alloy.

After the free tin is properly removed, the alloyed tin may be analyzed by one of the following procedures:

1. Dissolve the sample completely and determine the tin content of the solution by any of the available methods: however, a correction must be made for the tin in the steel. The Sellars' procedure is probably the most convenient and may be successfully used providing the strength of the iodate solution is decreased to give a reasonable titre with the small percentage of tin present. Occasionally steels are encountered in which the minor alloying elements, particularly copper, interfere with the titration end point.

2. The alloy is stripped and the tin determined by the Bendix method.

3. Total alloy, both tin and iron, can be quantitatively removed without attacking the underlying steel by immersing the sample in a solution of 5–10 per cent sodium hydroxide at 90°C, kept bubbling by dropwise additions of 30 per cent hydrogen peroxide. Alloy thickness is measured by loss in weight.

All of the methods described heretofore, if used for the determination of both free tin and alloy, are laborious and time consuming. The new method described in this paper is simple and quite rapid, and the free tin and alloy are ascertained in one operation.

Electrolytic Determination of Free and Alloyed Tin

The anodic dissolution of tin coatings on steel proceeds with full current efficiency in 1*N* HCl, enabling the coating weight of a defined area to be calculated from Faraday's Law. In contrast with the anodic stripping of tin in an alkaline electrolyte (4, 5), the action does not stop at the tin-iron alloy surface but removes this constituent as well. If the voltage which develops between the specimen (anode detinning at a constant current) and a reference electrode is measured on a recording potentiometer, a time-potential curve is obtained with two readily distinguishable end points from which the free and alloyed tin can be determined.

In seeking the proper electrolyte, which would satisfactorily remove the alloy, approximately 100 substances were investigated including practically all of the common salts of sodium, potassium, ammonium, and calcium, some organic and inorganic acids, and acid-salt mixtures. Only the halogen acids showed any promise and a 1:10 dilution of commercial reagent grade HCl was finally selected. The concentration, here about 1*N*, is not critical.

Tests can be run at room temperature and the electrolyte may be used repeatedly until excessive plating of tin on the cathode decreases the distance between the cathode and the anode. Approximately 150 samples representing 1200 in.² of surface of No. 50 electrolytic plate can be analyzed before the solution has to be replaced.

Description of Apparatus

The complete stripping circuit is shown in Fig. 2. A Leeds and Northrup Speedomax Type G recorder, voltage range 0–5 mv with a chart speed of 2 in./min, was used to measure the potential changes. The 7.5 v battery provides the constant booster potential required in series with that of the cell to assure a total potential which is positive to the recorder at all times. Resistances, R3 and R4, are employed as a voltage divider to adjust sensitivity to the scale dimensions desired. The reference electrode may be a saturated calomel half cell but a silver rod performs equally well and no salt bridge

problems are encountered. Its position in the cell is not critical.

The source of cell current is an electronically regulated d-c power supply designed to deliver a maximum current of 0.5 amp (Fig. 3). The output is

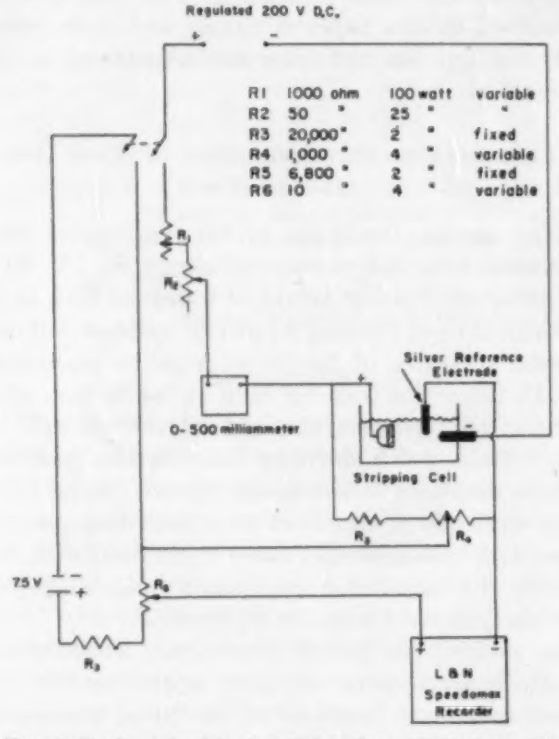
Regulated 200 V D.C.
R1 1000 ohm 100 watt variable
R2 50 " 25 " "
R3 20,000" 2 " fixed
R4 1,000 " 4 " variable
R5 6,800 " 2 " fixed
R6 10 " 4 " variable
Silver Reference Electrode
0- 500 milliammeter
Stripping Cell
75 V
L & N Speedomax Recorder

FIG. 2. Basic stripping circuit for electrolytic determinations of tin and tin-iron alloy coating weights on tin plate.

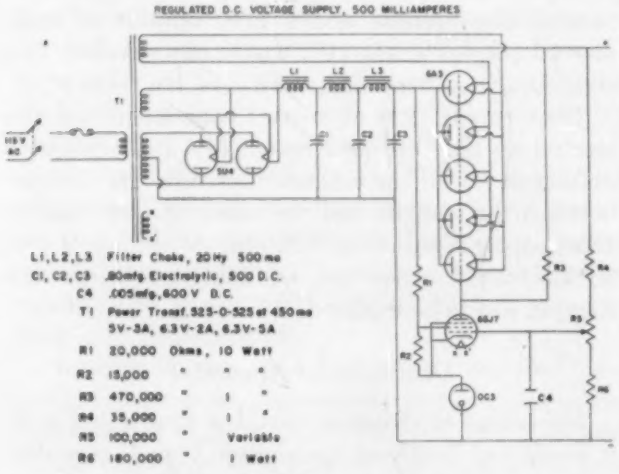
REGULATED D.C. VOLTAGE SUPPLY, 500 MILLIAMPERES
L1, L2, L3 Filter Choke, 20 Hy 500 ma
C1, C2, C3 .80mfg. Electrolytic, 500 D.C.
C4 .005mfg., 600 V D.C.
T1 Power Transf. 525-0-525 at 450 ma
5V-3A, 6.3V-2A, 6.3V-5A
R1 20,000 Ohms, 10 Watt
R2 15,000 " " "
R3 470,000 " 1 "
R4 35,000 " 1 "
R5 100,000 " Variable
R6 180,000 " 1 Watt

FIG. 3

200 v, which is subsequently suitably metered and regulated by the other components. This feature assures constant current during electrolysis since small potential changes across the cell are negligible compared to the output voltage. Satisfactory results have been obtained with a 45 v d-c source as supplied by twelve 45 v dry cells connected in parallel; however, these batteries polarize readily under high current drain and a constant stripping current cannot be maintained. This current source could be employed where electrolysis requires only low current densities.

The cell is a rectangular box, with inside dimensions of 4 x 4 x 6 in., constructed of acid-resistant bakelite. A stuffing box type of plug is provided at one end for insertion of the cathode, which is a ¼ in. carbon rod located centrally and at right angles to the plane of the anode. Cathode distance, approximately ¾ in., is adjusted to provide a current density distribution such that the rate of dissolution is equal at the edge and center, but greater than in annular area between. Location of the cathode at excessive distances from the anode results in a concentration of current at the edge, and alloy dissolves from the peripheral area prior to complete free tin removal at the center. The reverse effect is obtained with the cathode too near the anode, the

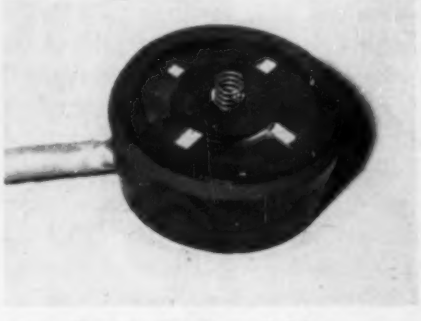

FIG. 4. Specimen holder

alloy dissolving prematurely from the center. The current density distribution is improved by covering the carbon rod with a snug gum rubber tube to within ⅛ in. of the tip.

The possibility of designing a more satisfactory cathode is recognized, and various configurations such as cones, disks, and rings have been investigated. None of these arrangements is superior to the carbon rod described.

The anode is a 4 in.² tin plate disk held in place by a specially designed vacuum holder which masks the back side from electrolytic action. The specimen holder shown in Fig. 4 is constructed from a No. 13 rubber stopper which contains two holes originating at the face and side respectively and meeting in the center of the stopper. A 9-in. length of ⅜-in. copper tube is inserted into the side opening. It provides both a current path and a means of applying the vacuum. The wide face of the stopper is channeled with four slots, ⅛ in. deep and ¾ in. in length, extending radially from the center opening. A rubber gasket, 1/16 in. thick with a 2 in. ID, is cemented to the outer edge, and in order to prevent the sample from buckling when vacuum is applied, a ring of the

same thickness, 1 in. in diameter with a ½ in. opening, is attached to the center of the stopper. A beryllium-copper spring, soldered to the copper tube, extends from the center of the stopper to conduct current to the specimen. That portion of the copper tube, which is immersed in the electrolyte, is coated with paraffin. Similar holders can be designed for smaller or larger circular specimens.

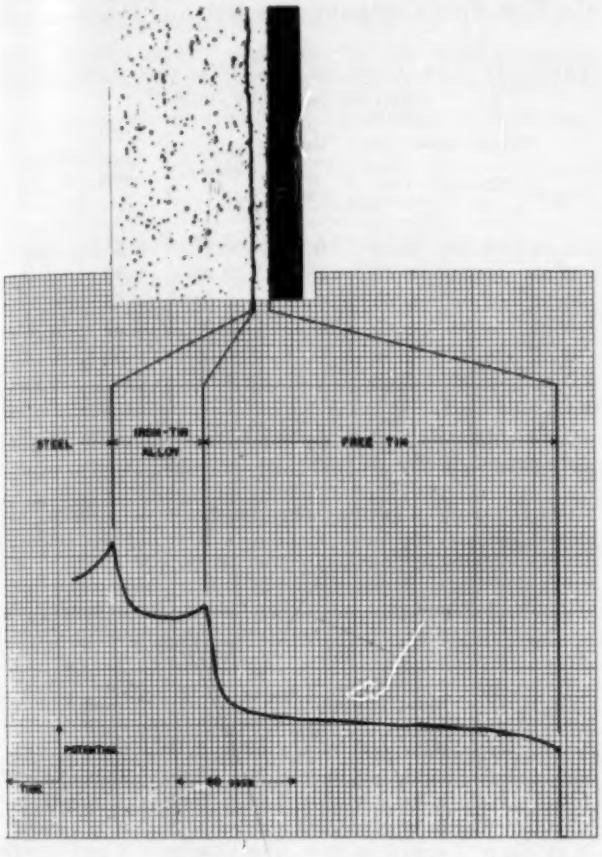

FIG. 5. Time-potential curve on hot-dipped plate, illustrating typical half-cell potential changes which occur during electrolytic removal of the tin coating.

Current Density Requirements

Anode efficiency remains constant over the range of current densities investigated, namely 100–500 ma/4 in.^{2} However, a few isolated instances have been encountered where the alloy is not attacked with 100 ma/4 in.^{2} but can be removed with the application of higher current densities. The most practical value appears to be 250 ma/4 in.^{2} since it produces a well proportioned time-potential curve and permits estimation of the removal time with an error not exceeding 1 per cent for thin electrodeposits. For heavier coatings this percentage error is correspondingly lower. Where very rapid analysis is desired higher current densities may be employed but extreme care must be exercised in positioning the cathode to prevent premature alloy dissolution. Smaller size samples can be analyzed with proportionately smaller currents.

Instrument Calibration

The precision of the electrolytic tester described depends to a considerable degree on the reliability of the component parts, particularly the milliammeter, and it is essential that the instrument be calibrated. This is best accomplished by determining the weight loss of pure tin specimens electrolyzed for a given time interval and expressing the results as milligrams or pounds of tin per base box per second. The meter used for the data reported gave a factor of 0.00535 lb/BB/sec with a setting of 250 ma when electrolyzing 4 in.^{2} samples.

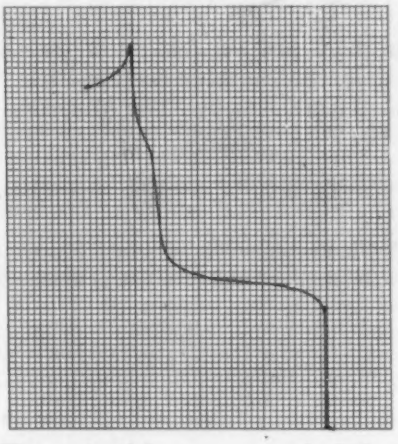

FIG. 6. Time-potential curve on nominal No. 50 electrolytic tin plate.

Operation of the Instrument

Prior to anodic stripping, the tin plate sample is cathodically treated in a 0.5 per cent sodium carbonate solution for 10 sec with a current density of 0.5 amp/in.^{2} This procedure reduces the tin oxide, present on the surface, to metallic tin and greatly improves the definition of the end points. The sample is blotted to remove excess moisture and affixed to the specimen holder by applying a vacuum (approximately 25 in. Hg gauge). After insertion in the cell, the stripping circuit is closed and the recorder automatically plots the time-potential curve. Photographs of actual curves shown in Fig. 5 and 6 typify the results obtained on common coke[4] hot dipped and No. 50 electrolytic tin plate respectively. The photomicrograph in Fig. 5 illustrates the relative thickness of the constituents which comprise the tin coating.

[4] Common cokes—AISI terminology for that grade of hot-dipped plate which, over an extended period, will consume 1.25 lb tin/BB from the tin pot and will carry an average coating weight of 1.10 lb tin/BB.

The time for removal of the free tin, obtained from the curve, is converted to the conventional coating weight designation by the following calculation:

$$\text{time} \times 0.00535 = \text{lb tin/BB.}$$

Since the tin-iron alloy composition is $FeSn_2$ and these elements enter the solution stoichiometrically with a two electron loss for each atom of tin and iron, only two thirds of the current is utilized for the dissolution of tin. Consequently the total alloy time must be corrected to compensate for the electrolysis of the iron. The theoretical factor is 0.67; however, on the basis of extensive investigation, comparing the actual tin content of the alloy to the removal time, the authors believe that 0.65 is a more representative figure. The alloyed tin is thus obtained from the formula:

$$\text{time} \times 0.65 \times 0.00535 = \text{lb/BB.}$$

Summation of the free and alloyed tin gives the total amount of tin in the coating. These calculations

TABLE I. *Free tin determinations by acid electrolysis and Sellars' wet chemistry procedure, lb/BB**

	HCl electrolysis	Sellars
Common coke	0.80	0.80
No. 50 Electrolytic	0.42	0.42
No. 25 Electrolytic	0.20	0.20

* Average of three specimens

can be simplified by designing a sliding scale or constructing a table or graph of time vs. coating weight.

Comparison of Electrolytic Stripping Procedure With Other Methods of Analysis

In order to verify the results of hydrochloric acid electrolysis, a number of comparisons were made with other methods of analysis. The first of these involved only the free tin portion of the coating. A special cell was designed so that the solution in which the free tin was anodically dissolved could be analyzed by the Sellars procedure (1). A direct comparison on the same specimen was therefore possible. Typical results, obtained in this manner, are given in Table I for three weights of tin coating.

A more complete evaluation was subsequently conducted to include free and alloyed tin and also the total amount of tin in the coating. Methods of analysis were acid and alkaline electrolytic stripping and Sellars'. Typical data on six No. 50 electrolytic tin plates are summarized in Table II with each value representing the average of six determinations.

A joint project was undertaken to compare the results of acid electrolysis with those obtained by the nondestructive x-ray absorption method. X-ray determinations were made on 4 in.^{2} disks of common coke hot dipped and No. 50 electrolytic tin plate by the U. S. Steel Company Research and Development

TABLE II. *Acid electrolysis vs. alkaline electrolysis and wet chemistry procedure, lb/BB*

HCl electrolysis			NaOH electrolysis, free tin	Sellars', alloyed tin	Total* coating	Sellars', total coating
Free tin	Alloyed tin	Total coating				
0.44	0.10	0.54	0.43	0.11	0.54	0.54
0.40	0.03	0.43	0.39	0.03	0.42	0.44
0.52	0.04	0.56	0.51	0.04	0.55	0.56
0.43	0.06	0.49	0.43	0.06	0.49	0.50
0.41	0.09	0.50	0.41	0.09	0.50	0.51
0.43	0.06	0.49	0.42	0.06	0.48	0.49

* Summation of free tin by NaOH electrolysis and alloyed tin by Sellars' procedure.

TABLE III. *Tin coating determinations on identical tin plate specimens by nondestructive x-ray and hydrochloric acid electrolytic methods, lb/BB*

No. 50 Electrolytic				Common coke hot dipped			
Electrolytic			X-ray	Electrolytic			X-ray
Free tin	Alloyed tin	Total coating	Total coating	Free tin	Alloyed tin	Total coating	Total coating
0.42	0.06	0.49	0.50	0.82	0.16	0.98	0.98
0.43	0.07	0.50	0.51	0.89	0.19	1.08	1.08
0.44	0.06	0.50	0.49	0.84	0.18	1.02	1.02
0.44	0.06	0.50	0.50	0.75	0.17	0.92	0.92
0.43	0.07	0.50	0.50	0.92	0.20	1.12	1.12
0.43	0.06	0.49	0.49	0.71	0.19	0.90	0.91
0.43	0.07	0.50	0.50	0.98	0.20	1.18	1.16
0.44	0.06	0.50	0.51	0.96	0.18	1.14	1.12
0.42	0.07	0.49	0.50	0.67	0.17	0.84	0.83
		—	—	0.88	0.19	1.07	1.07
	Avg	0.50	0.50	0.82	0.20	1.02	1.02
				0.72	0.19	0.91	0.91
				0.77	0.18	0.95	0.95
				0.70	0.18	0.88	0.89
						—	—
					Avg	1.01	1.01

Laboratory, Pittsburgh, Pa., and the same samples forwarded to the American Can Company Laboratory for electrolytic analysis. The results are given in Table III.

Limitations

The electrolytic tester determines the tin coating on one side of the plate. This has certain advantages when investigating the effect of tin on corrosion resistance since a given plate does not necessarily

have identical coating weights on both sides. If the total tin coating weight is desired, it is obvious that two separate single side analyses are required. Attempts have been made to devise a satisfactory procedure for determining both sides simultaneously, but results to date have not been very encouraging. Unequal amounts of tin result in alloy dissolution on the lower coated side while free tin is present on the reverse face, consequently the time-potential curves have additional and indistinct end points. It is quite possible that this problem could be surmounted.

Conclusions

A new electrolytic procedure for determination of tin on tin plate was described which may be employed with confidence to replace any of the present methods of tin coating analysis. The distinguishing feature is the estimation of free and alloyed tin in a single operation. This measure of alloy thickness surpasses other methods in reliability and speed. This method should find extensive use with the advent of "differential"[5] coated tin plates which were developed to conserve tin.

Acknowledgments

The authors wish to express their appreciation to Mr. R. R. Hartwell and Dr. L. P. Gotsch for their helpful criticisms and suggestions in this investigation. Acknowledgment is also due to the management of the U. S. Steel Company for permission to publish the x-ray tin coating data.

References

1. "Scott's Standard Methods of Chemical Analysis," 5th ed., Vol. **1**, p. 966, D. Van Nostrand Co., New York (1939).
2. G. H. Bendix, W. C. Stammer, and A. H. Carle, *Ind. and Eng. Chem., Anal. Ed.*, **15**, 501 (1943).
3. S. G. Clarke, *Analyst*, **59**, 525 (1934).
4. H. T. Francis, *Trans. Electrochem. Soc.*, **93**, 79 (1948).
5. A. W. Hothersall and W. N. Bradshaw, *J. Iron Steel Inst. (London)*, **133**, 225 (1936).
6. H. F. Beeghly, *J. Electrochem. Soc.*, **97**, 152 (1950).

[5] Designation applied to tin plates electrocoated with different amounts of tin on opposite surfaces.

Role of Crystal Orientation in the Oxidation of Iron[1]

EARL A. GULBRANSEN AND ROSWELL RUKA

Westinghouse Research Laboratories, East Pittsburgh, Pennsylvania

ABSTRACT

The interface between a metal and its oxide or other corrosion films is a zone of great interest in the general phenomena of protection of metals. The system of iron and its oxides is considered in this work. Experiments are made using the electron diffraction high temperature camera on the oxidation of single crystals of iron. Definite orientation effects are found between the metal and the oxide if the oxidation is carried out slowly, for example, in a 50 per cent H_2O-50 per cent H_2 mixture at 750°C or in high vacuum. Rapid oxidation shows that the original orientation effects are not carried through to thick films.

The orientation effects are interpreted in terms of two principles: (*a*) the conservation of similar repeat distances in the two lattices and (*b*) conservation of atom density. The effect of the forward and reverse solid phase reaction $Fe_3O_4 + Fe \rightarrow 4FeO$ is studied and it is shown that the orientation effects are carried through to the newly formed oxide. The results are discussed in their relationships to the general phenomena of oxidation and corrosion.

INTRODUCTION

The phenomena occurring at the interface between a metal and its oxide during the course of a chemical reaction with oxygen are of great interest in the understanding of the mechanism of the reaction. Since the metal and the oxide differ in their crystal structures, a transition zone must exist between the two structures. From energy and entropy considerations alone it may be expected that certain planes of the oxide may grow preferentially on a given plane of the metal. In this way the oxide may have varying degrees of orientation depending upon energy conditions between the two structures, the rate of chemical reaction, and the nature of the oxidizing atmosphere.

The mutual orientation of two different crystal structures when one is formed upon the other is called "epitaxie." For the historical development of these concepts one may refer to the work of Royer (1).

It is the purpose of this paper to determine the mutual orientation of FeO and Fe_3O_4 oxide films or scales on iron when formed under varying oxidation conditions. These conditions include the following variables: (*a*) nature of the oxidizing atmosphere, (*b*) time of oxidation, (*c*) pressure, (*d*) temperature, and (*e*) heating and cooling cycles. The following problems will be studied: (*a*) the mutual orientation between α-Fe and "FeO," Wustite, as a result of oxidation in H_2O-H_2 mixtures above 570°C, (*b*) the mutual orientation between Fe and Fe_3O_4 as a result of oxidation in H_2O-H_2 mixtures below 570°C, (*c*) effect of pretreatment of the specimen on orientation of the oxide, (*d*) the mutual orientation between α-Fe and Fe_3O_4, and α-Fe and "FeO" as a result of oxidation in high vacuum below 600°C, (*e*) the mutual orientation between α-Fe and the system of oxides formed by oxidation in oxygen atmospheres above 570°C, and (*f*) the mutual orientation between α-Fe, "FeO," and Fe_3O_4 in the forward and reverse solid phase reaction, α-Fe + $Fe_3O_4 \rightleftharpoons$ 4"FeO."

Epitaxie in Metal-Oxide Systems

Oxide orientation relationships involving Ba, Ni, Zn, Wo, Al, Cu, and several forms of Fe have been studied by various investigators under many different conditions (2–12, 31, 32).

Electron Diffraction Method

Interpretation of electron diffraction patterns was made using reciprocal lattice networks, which are particularly convenient for use with electron diffraction studies. The method has been applied to electron diffraction in a number of cases (7, 13–21) based on fundamental theory (22, 23).

SAMPLES AND APPARATUS

The samples were prepared from Puron grade iron. An analysis of this material indicated that no metallic impurity was present to more than 0.0015 per cent. The chief impurity was oxygen, 0.04 per cent. Carbon was present to 0.005 per cent. Rods of this material were annealed in H_2 at 875°C which reduced the oxygen content so that the final analysis was 99.98+ per cent Fe.

The strain-anneal method was used to prepare single crystals. Five-mil strips were given an anneal in a vacuum of 10^{-6} mm of Hg or less at 875°C for

[1] Manuscript received July 23, 1951.

24 hours. The strips were stretched slowly to an elongation of 5 per cent over a period of 30 minutes, then annealed in high vacuum for 48 hours at 875°C.

The strips were etched in nital which exposes the (100) faces, and similarly oriented crystals were identified by observations with a two-circle optical goniometer. The single crystals varied from 2 to 10 mm on an edge. Specimens 0.475 cm in diameter were punched from the single crystals. The strips consisted of (100), (211), and (311) planes on the surface.

Orientations of the specimens were determined, after etching in nital, with an electron microscope[2] using a diffraction adapter. These were checked in some cases by x-ray diffraction patterns. Specimens were rotated in the apparatus while diffraction patterns were observed on the fluorescent screen. Thus, a particular cross array of spots could be identified and orientation marked on the specimen.

A high temperature electron diffraction camera (25, 26) was used for all experiments. By choosing suitable beam apertures it was possible to study the diffraction pattern visually on the fluorescent screen. Photographs were made at critical points for detailed study.

Results and Discussion

Mutual Orientation of α-Fe-"FeO" *above 570°C* (H_2O-H_2 *Mixtures*)

The orientation relationship between α-Fe and "FeO" was determined by oxidation of etched specimens in 50 per cent H_2O-50 per cent H_2 mixtures. Thermodynamic considerations indicated that "FeO," Wustite, was the stable oxide at 650° and 750°C in this atmosphere (24). Single crystals of α-Fe having the free surface planes of (100), (211), and (311) were studied.

A cross array of spots is observed in the different patterns in Fig. 1-1 and 1-2. A plot of the spots indicates a diagonal section through the origin of the reciprocal lattice representation. An unusual feature of these photographs is that the spots have long tails in a direction perpendicular to the shadow edge. These tails appear to be associated with the thin initial oxide film formed on the surface and indicate a relaxation of both the X and Z diffraction conditions.

In Fig. 1 patterns 3 and 4 show double spots or arcs and indicate highly oriented crystals of "FeO."

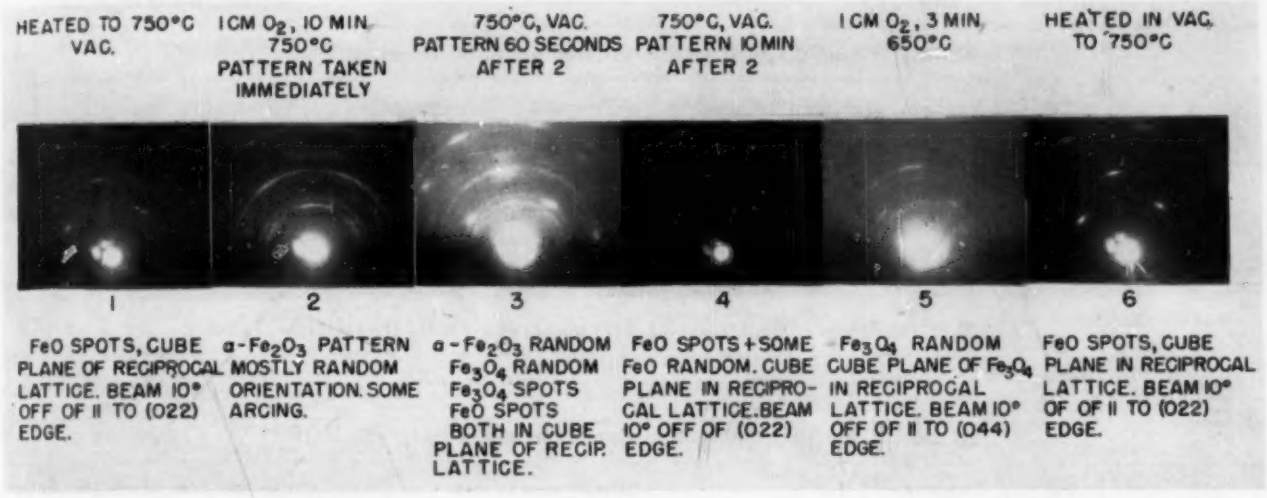
HEATED TO 750°C VAC.
1CM O_2, 10 MIN. 750°C PATTERN TAKEN IMMEDIATELY
750°C, VAC. PATTERN 60 SECONDS AFTER 2
750°C, VAC. PATTERN 10 MIN AFTER 2
1CM O_2, 3 MIN. 650°C
HEATED IN VAC. TO 750°C
1
2
3
4
5
6
FeO SPOTS, CUBE PLANE OF RECIPROCAL LATTICE. BEAM 10° OFF OF ‖ TO (022) EDGE.
α-Fe_2O_3 PATTERN MOSTLY RANDOM ORIENTATION. SOME ARCING.
α-Fe_2O_3 RANDOM Fe_3O_4 RANDOM Fe_3O_4 SPOTS FeO SPOTS BOTH IN CUBE PLANE OF RECIP. LATTICE.
FeO SPOTS + SOME FeO RANDOM. CUBE PLANE IN RECIPROCAL LATTICE. BEAM 10° OFF OF (022) EDGE.
Fe_3O_4 RANDOM CUBE PLANE OF Fe_3O_4 IN RECIPROCAL LATTICE. BEAM 10° OFF OF ‖ TO (044) EDGE.
FeO SPOTS, CUBE PLANE IN RECIPROCAL LATTICE. BEAM 10° OF OF ‖ TO (022) EDGE.

FIG. 1. Orientation relationships α-Fe-"FeO," α-Fe-Fe_3O_4, and Fe_3O_4-"FeO"-oxidation of original (100) plane of α-Fe by H_2-H_2O mixture.

This may be interpreted as indicating that the oxide forming on the single crystal of metal is not a single crystal of "FeO" but rather a large number of crystallites aligned in an angular region around a given orientation. The effect of time of oxidation is to change the two-spot structure to a simple arc.

Fig. 1, pattern 5 shows the diffraction pattern formed on cooling "FeO" through its transformation temperature where it is changed to Fe_3O_4. The spots corresponding to the Fe_3O_4 film are arcs indicating a highly oriented film of Fe_3O_4 crystallites. Fig. 1, pattern 6 shows the diffraction pattern on reheating the specimen in vacuum to 650°C. The transformation to "FeO" occurs during the heating cycle.

Tables I and II summarize experimental results for oxidation of the three crystal faces at 650° and 750°C. In all cases a cube direction [010] of "FeO" or Fe_3O_4 is found to lie parallel to the [110] direction of α-Fe. These results confirm the work of other investigators (2, 31).

[2] Of the type RCA E.M.B.

TABLE I. *Oxidation (100), (211), and (311) planes of* α-Fe, H_2-H_2O *mixture, 650°C*

Pattern No.	Temp °C	Oxidation conditions	Crystal structure	Orientation of oxide, reciprocal lattice representation
		A. (100) Plane, diagonal section through origin of reciprocal lattice		
1	485	Vacuum	α-Fe spots	
2	650	Vacuum	α-Fe spots	
3	650	0.7 cm H_2O + 0.7 cm H_2, 1 minute	"FeO" spots, spots are doubled	Cube section through origin, (100) plane in surface
4	650	0.7 cm H_2O + 0.7 cm H_2, 60 minutes	"FeO" spots, spots are arced	Cube section through origin, (100) plane in surface
		B. (211) Plane, diagonal section through origin of reciprocal lattice		
1	650	Vacuum	α-Fe spots	
2	650	0.3 cm H_2O + 0.3 cm H_2, 1 minute	"FeO" spots	Cube section through origin, ≈ (110) plane in surface
3	650	0.3 cm H_2O + 0.3 cm H_2, 30 minutes	"FeO" spots	Cube section through origin, ≈ (110) plane in surface
		C. (311) Plane, diagonal section through origin of reciprocal lattice		
1	750	Vacuum, specimen reduced in H_2	α-Fe spots	
2	650	0.3 cm H_2O + 0.3 cm H_2, 1 minute	"FeO" arced spots + small amount random	Cube section through origin, (310) plane in surface
3	650	0.3 cm H_2O + 0.3 cm H_2	"FeO" arced spots + small amount random	Cube section through origin, (310) plane in surface

TABLE II. *Oxidation (100), (211), and (311) planes of* α-Fe, H_2-H_2O *mixture, 750°C*

Pattern No.	Temp °C	Oxidation conditions	Crystal structure	Orientation of oxides, reciprocal lattice representation
		A. (100) Plane, diagonal section through origin of reciprocal lattice		
1	750	Vacuum	"FeO" spots	Cube section through origin, (100) plane on surface
2	750	0.7 cm H_2O + 0.7 cm H_2, 1 minute	"FeO" spots	Cube section through origin, (100) plane on surface
3	750	0.7 cm H_2O + 0.7 cm H_2, 10 minutes	"FeO" spots	Cube section through origin, (100) plane on surface
4	750	0.7 cm H_2O + 0.7 cm H_2, 60 minutes	"FeO" spots	Cube section through origin, (100) plane on surface
5	750	Heated in vacuum, 60 minutes more	"FeO" spots	Cube section through origin, (100) plane on surface
		B. (211) Plane, diagonal section through origin of reciprocal lattice		
1	750	Vacuum, specimen reduced in H_2	α-Fe spots	
2	750	0.3 cm H_2 + 0.3 cm H_2O, 1 minute	α-Fe spots + Fe_3O_4 spots	Cube section through origin, ≈ (110) plane on surface
3	750	0.3 cm H_2 + 0.3 cm H_2O, 20 minutes	"FeO" spots + slight random pattern	Cube section through origin, ≈ (110) plane on surface
		C. (311) Plane, diagonal section through origin of reciprocal lattice		
1	550	Vacuum	α-Fe spots + "FeO" spots	Cube section through origin, (310) plane on surface
2	750	0.3 cm H_2O + 0.3 cm H_2, 1 minute	"FeO" spots	Cube section through origin, (310) plane on surface
3	750	0.3 cm H_2O + 0.3 cm H_2	"FeO" spots + slight random pattern	Cube section through origin, (310) plane on surface

Effect of Pretreatment on Orientation of Oxide with the Metal (above 570°C)

Two effects are studied: (*A*) the orientation produced on a polished and annealed specimen, and (*B*) the effect of hydrogen reduction of the surface oxide on the orientation of "FeO" produced in subsequent oxidation.

A. Polished and annealed specimen.—Since etching in nital not only exposes (100) faces but may also leave traces of impurities on the surface, an alternative procedure was used for removing the disordered surface crystals produced by the abrading procedure. One sample was abraded with 4/0 polishing paper and then annealed for 60 hours at 850°C in a vacuum of about 10^{-5} mm of Hg. This specimen, having originally the (211) plane on the surface, showed an oriented pattern of "FeO" on heating to 650°C. The cross array of spots was identical with that found on oxidation in H_2O-H_2 mixtures of the etched (211) surface of α-Fe. Further oxidation in H_2O-H_2 mixtures showed similar diffraction patterns.

It was concluded that the disordered surface crystals were oriented to the original α-Fe orientation by the long anneal and that the "FeO" crystals formed by vacuum oxidation arranged themselves in the characteristic orientation for this surface.

B. Reduction by dry H_2.—The specimen described in *A*, having an oriented layer of "FeO" crystallites, was next exposed to H_2 at 1 cm of Hg pressure for 2 minutes. After evacuation, the diffraction pattern showed a mixture of α-Fe and "FeO" spots with the α-Fe having the orientation of the base metal (211) and the "FeO" having the same orientation as before treatment with H_2. Subsequent oxidation in H_2O-H_2 mixtures gave the characteristic orientation of "FeO" for this surface of α-Fe.

Mutual Orientation α-Fe *and* Fe_3O_4 *Below 570°C* (H_2O-H_2 *Mixtures*)

To avoid formation of an "FeO" layer between α-Fe and Fe_3O_4 as well as formation of α-Fe_2O_3 in contact with Fe_3O_4, it was essential to study the oxidation below 570°C and in H_2O-H_2 mixtures. α-Fe_2O_3 was readily reduced to Fe_3O_4 by H_2 at 400°C if the partial pressure ratio of H_2O/H_2 was maintained below 173000/1 while Fe_3O_4 was not reduced by H_2 if the H_2O/H_2 ratio was maintained greater than 1/6.72. Mixtures of H_2O and H_2 of 50 per cent H_2O-50 per cent H_2 up to 90 per cent H_2O-10 per cent H_2 were used in these experiments.

Oxidation experiments were made on the three single crystals in H_2O-H_2 mixtures in the temperature range of 300° to 500°C. Table III shows results for oxidation of the (100) plane of α-Fe at 300° and 500°C and the (211) and (311) planes at 400°C. All patterns of Fe_3O_4 show orientation effects and the

TABLE III. *Oxidation (100), (211), and (311) planes of* α-Fe, H_2-H_2O *mixtures below 570°C*

Pattern No.	Temp °C	Oxidation conditions	Crystal structure	Orientation of oxide in reciprocal lattice
A. (100) Plane, diagonal section through origin in reciprocal lattice of α-Fe, 300° and 500°C				
1	300	Vacuum	α-Fe spots, trace random Fe_3O_4	
2	300	0.4 cm H_2O + 0.35 cm H_2, 15 minutes	Slight random Fe_3O_4, weak Fe_3O_4 spots	Cube section through origin, (100) plane in surface
3	300	0.45 cm H_2O + 0.35 cm H_2, 20 minutes additional	Random Fe_3O_4, Fe_3O_4 spots	Cube section through origin, (100) plane in surface
4	500	0.45 cm H_2O + 0.35 cm H_2, 10 minutes additional	Fe_3O_4 spots, weak random Fe_3O_4	Cube section through origin, (100) plane in surface
5	545	Vacuum	Fe_3O_4 spots, trace random Fe_3O_4	Cube section through origin, (100) plane in surface
B. (211) Plane, diagonal section through origin in reciprocal lattice of α-Fe, 400°C				
1	400	Vacuum, reduced in H_2	α-Fe spots + Fe_3O_4 spots	Cube section through origin, ≈ (110) plane in surface
2	400	0.3 cm H_2O + 0.3 cm H_2, 1 minute	Fe_3O_4 spots + trace α-Fe spots	Cube section through origin, ≈ (110) plane in surface
3	400	0.9 cm H_2O + 0.1 cm H_2, 20 minutes	Fe_3O_4 spots	Cube section through origin, ≈ (110) plane in surface
C. (311) Plane, diagonal section through origin in reciprocal lattice of α-Fe, 400°C				
1	650	Vacuum, reduced in H_2	α-Fe spots	
2	400	0.4 cm H_2O + 0.1 cm H_2, 20 minutes	Fe_3O_4 spots + trace random Fe_3O_4	Cube section through origin, (310) plane in surface

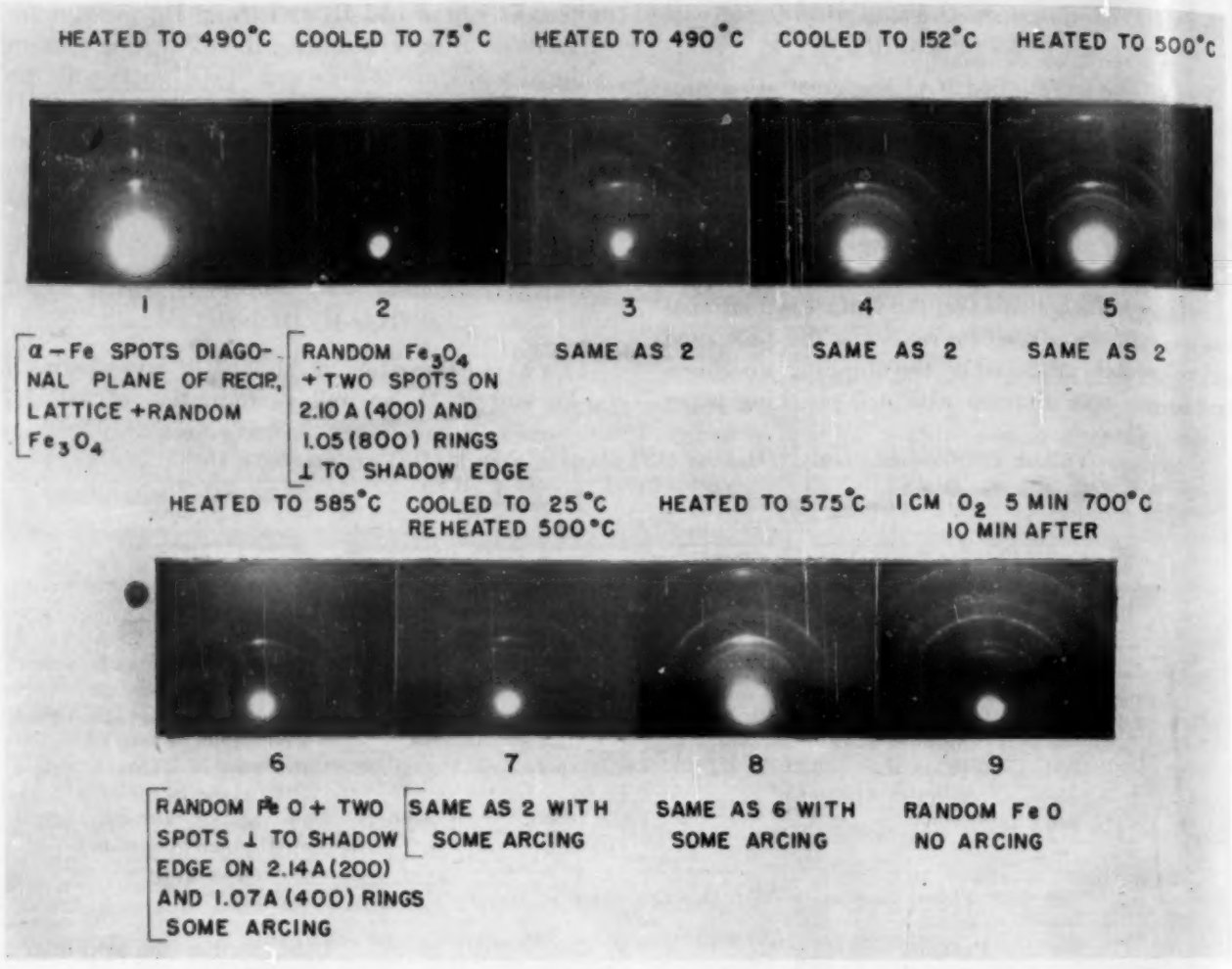
HEATED TO 490°C
COOLED TO 75°C
HEATED TO 490°C
COOLED TO 152°C
HEATED TO 500°C
1
2
3
4
5
α–Fe SPOTS DIAGONAL PLANE OF RECIP. LATTICE +RANDOM Fe_3O_4
RANDOM Fe_3O_4 + TWO SPOTS ON 2.10 A (400) AND 1.05 (800) RINGS ⊥ TO SHADOW EDGE
SAME AS 2
SAME AS 2
SAME AS 2
HEATED TO 585°C
COOLED TO 25°C
REHEATED 500°C
HEATED TO 575°C
1 CM O_2 5 MIN 700°C
10 MIN AFTER
6
7
8
9
RANDOM FeO + TWO SPOTS ⊥ TO SHADOW EDGE ON 2.14 A (200) AND 1.07 A (400) RINGS SOME ARCING
SAME AS 2 WITH SOME ARCING
SAME AS 6 WITH SOME ARCING
RANDOM FeO NO ARCING

FIG. 2. Mutual orientation α-Fe and Fe_3O_4, and "FeO"-vacuum oxidation below 600°C (100) plane of α-Fe

TABLE IV. *Oxidation (211) surface of* α-Fe *low pressure* O_2, *650°C*

Pattern No.	Temp °C	Oxidation conditions	Crystal structure	Orientation of oxide, reciprocal lattice representation
		A. (211) Plane in surface, diagonal plane through origin of reciprocal lattice		
1	400	Vacuum	α-Fe spots	
2	650	1 mm O_2, 1 minute	Random "FeO"	None
3	650	1 cm O_2, 19 minutes additional	Random "FeO"	None
4	650	1 cm O_2, 2 minutes additional	Random α-Fe_2O_3	None
5	650	Vacuum, 10 minutes after 4	Random "FeO"	None
6	115	Vacuum	Random Fe_3O_4	None
		B. (100) Plane in surface, diagonal section through origin of reciprocal lattice		
1	650	Vacuum	Random "FeO" + "FeO," arced spots	Cube section through origin, (100) plane in surface
2	650	0.1 mm O_2, 1 minute	Random "FeO" + "FeO," arced spots	Cube section through origin, (100) plane in surface
3	650	0.1 mm O_2, 10 minute total	Random "FeO" + weak "FeO," arced spots	Cube section through origin, (100) plane in surface
4	650	1.0 mm O_2, 1 minute	Weak random "FeO" + weak "FeO," arced spots	Cube section through origin, (100) plane in surface
5	650	1.0 cm O_2, 1 minute	Weak random "FeO" + weak "FeO," arced spots	Cube section through origin, (100) plane in surface
6	650	1.0 cm O_2, 20 minutes	Strong random α-Fe_2O_3 + Fe_3O_4	None

orientation relationships observed are identical with those found for "FeO" at 650° and 750°C.

Mutual Orientation α-Fe-Fe_3O_4 and α-Fe-FeO-Vacuum Oxidation Below 600°C

It has been noted previously that oxidation of single crystal sheets of α-Fe at temperatures of 200° to 500°C produces completely random oxide patterns over a comparatively wide range of oxide thicknesses. These observations appear to differ with experiments of Nelson (31) on evaporated iron films.

The growth of orientation was studied under what appeared to be the best conditions outside of the H_2O-H_2 atmosphere. Oxidation occurred under vacuum conditions of the order of 10^{-5} mm of Hg or lower with a relatively low rate of attack and under conditions where α-Fe_2O_3 was not formed.

Fig. 2 illustrates the smaller orientation effects encountered on heating and cooling a vacuum-formed oxide film (10^{-5} mm of Hg) on the (100) plane of an α-Fe specimen etched in nital. The tendency to form an oriented pattern increased with time and with the number of heating and cooling cycles.

A similar behavior, except for a slower vacuum oxidation, was observed for a similarly prepared (211) plane of α-Fe. Long heating of another sample produced a greater amount of orientation approaching that found in the H_2O-H_2 oxidations.

α-Fe spots initially present in these experiments were observed to develop "tails" in a line perpendicular to the shadow edge. These disappeared as the oxide pattern became predominant.

The small amount of orientation that was present in these experiments was consistent with that observed for the H_2O-H_2 oxidation.

Slow oxidation under vacuum conditions below 570°C did not form the highly oriented layers of Fe_3O_4 which were formed by the H_2O-H_2 mixtures at the same temperatures. Some arcing was noted in the patterns and the oxides did orient to some extent with the underlying metal and in the same direction as found with the H_2O-H_2 mixtures. Oxidation at 700°C gave an essentially random "FeO" structure although some orientation carry-over was noticed when the specimen was heated at 700°C for several hours and reoxidized. It is concluded that formation of completely oriented patterns in vacua at temperatures of the order of 600°C is a slow process compared to the results obtained with H_2O-H_2 mixtures.

Mutual Orientation of α-Fe and the Iron Oxides Formed by Oxidation in O_2 Above 570°C

Two types of surfaces will be compared: a specimen having the (211) plane in the surface but free from the presence of an oriented oxide film, and a specimen having the (100) plane in the surface and previously oxidized in H_2O-H_2 mixtures to form a highly oriented "FeO" film.

Orientation of the surface of the first specimen was checked by taking a diffraction pattern at 400°C during the heating cycle. The specimen was next heated to 650°C and a number of oxidation experiments made. Table IVA shows the results for several oxidation experiments. The solid phase reaction of $Fe_3O_4 + Fe \rightarrow 4$"FeO" was allowed to take place before the diffraction patterns were photographed, except in pattern 4. Completely random patterns of "FeO" are observed. Pattern 4 shows a random pattern of α-Fe_2O_3 since the picture was taken immediately after evacuation.

No orientation effects were observed for conditions studied. Long periods of heating or oxidation might aid the formation of an oriented film or scale.

The second specimen, having the (100) plane in the surface was oxidized in a 50%H_2O-50%H_2 mixture at 650°C to form a highly oriented film of "FeO." The specimen was cooled to room temperature and upon heating to 650°C a pattern of "FeO" arced spots was obtained together with a random pattern of "FeO." Table IVB describes a series of oxidation experiments at 650°C for several oxidation times and pressures. The influence of the oriented layer of "FeO" was important in the growth of the additional oxide layer since the arced spot pattern was present in the patterns, with the exception of pattern 6. Here the solid-phase reaction had not taken place.

This experiment leads to the conclusion that presence of an oriented layer of oxide aids formation of additional oriented layers.

Mutual Orientation—Solid Phase Reactions of Fe with the Higher Oxides Above 570°C

It has been shown (27) that when α-Fe is oxidized above 570°C the oxides Fe_3O_4 and α-Fe_2O_3 are formed in the outer layers of the oxide film or scale. The following reactions occur continually in the oxide above 570°C:

$$4\alpha\text{-}Fe_2O_3 + Fe \rightarrow 3Fe_3O_4 \qquad (I)$$

and

$$Fe_3O_4 + Fe \rightarrow 4\text{"FeO."} \qquad (II)$$

If the system is evacuated the higher oxides are completely reduced to "FeO" at 750°C in a few minutes.

A specimen, having the (211) plane in the surface, was oxidized in a H_2O-H_2 mixture to form a highly oriented layer of "FeO." Orientation relationships of the metal to the oxide were the same as those listed in Tables I and II. The specimen was placed

in a diffraction camera and heated to 750°C in vacuo. The two experiments illustrated in Fig. 3 show that the original oriented "FeO" layer determined final orientation of the additional oxide layer formed in oxidation. The rate of formation of the oriented layer from the unoriented higher oxides appeared to be of the same order as the rate of reduction of the higher oxides by iron. Thus, formation of the oriented layer seems to occur by diffusion of iron through the "FeO" film to the "FeO"-Fe_3O_4 interface where reaction with Fe_3O_4 occurs to form "FeO," the "FeO" being laid down on the original "FeO" structure.

Orientation relationships between α-Fe and "FeO" and Fe_3O_4 spots are the same as have been previously noted for Tables I and II for the (211) plane of α-Fe.

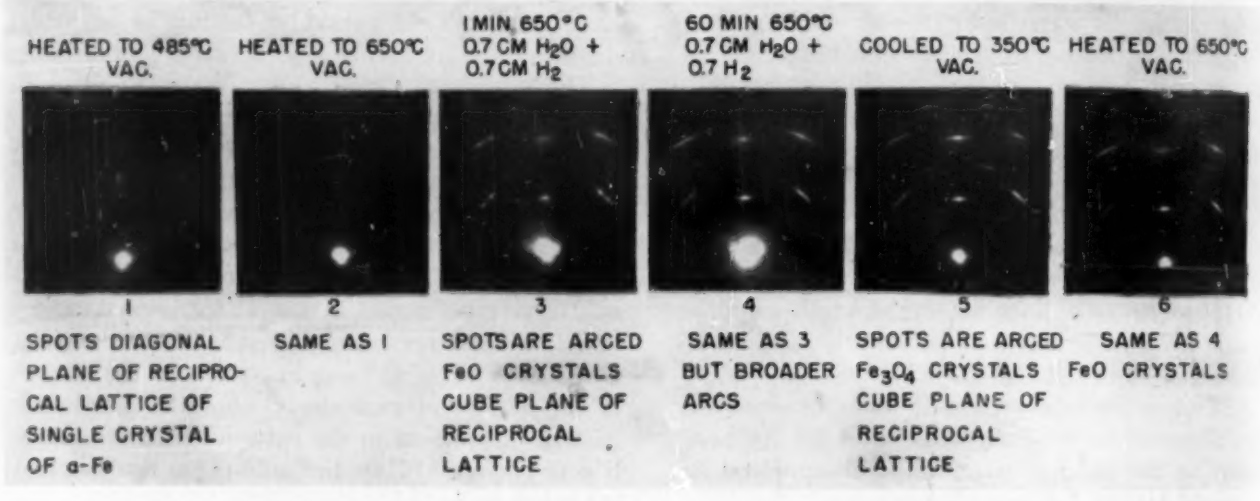
HEATED TO 485°C VAC.
HEATED TO 650°C VAC.
1 MIN 650°C 0.7 CM H_2O + 0.7 CM H_2
60 MIN 650°C 0.7 CM H_2O + 0.7 H_2
COOLED TO 350°C VAC.
HEATED TO 650°C VAC.
1
2
3
4
5
6
SPOTS DIAGONAL PLANE OF RECIPROCAL LATTICE OF SINGLE CRYSTAL OF α-Fe
SAME AS 1
SPOTS ARE ARCED FeO CRYSTALS CUBE PLANE OF RECIPROCAL LATTICE
SAME AS 3 BUT BROADER ARCS
SPOTS ARE ARCED Fe_3O_4 CRYSTALS CUBE PLANE OF RECIPROCAL LATTICE
SAME AS 4 FeO CRYSTALS

FIG. 3. Orientation relationships (*a*) oxidation of α-Fe (211) plane and (*b*) solid phase reaction of Fe with α-Fe_2O_3 and Fe_3O_4

DISCUSSION

Orientation Relationships

Orientation relationships between α-Fe and "FeO" and between "FeO" and Fe_3O_4 found by Mehl and McCandless (2) are confirmed in this study. They suggest that the face-centered tetragonal structure contained within the body-centered structure of α-Fe having an axial ratio $c:a$ equal to $1:\sqrt{2}$ expands to form the face-centered cubic lattice of iron atoms in "FeO" with an axial ratio of unity.

The present studies of α-Fe-Fe_3O_4 mutual orientation show similar orientation relationships to that for α-Fe-"FeO" for the three surfaces of α-Fe. The cube plane of Fe_3O_4 grew on the cube plane of α-Fe with the [010] direction of Fe_3O_4 parallel to the [110] direction of α-Fe.

Orientation relationships between Fe_3O_4 and "FeO" are such that one structure transforms into the other with a conservation of the original orientation. This may be expected from the similarity in crystal structures as noted by Goldschmidt (28).

Conditions for Producing Oriented Oxide Films

There are several possible reasons for the formation of highly oriented oxide films by H_2O-H_2 oxidation atmospheres even though oxidation in vacuo and in oxygen atmospheres produced only slightly oriented films unless these films were heated for long periods of time in high vacuo.

The fact that an oxide film is made up of many small crystallites on each grain of metal has been studied in some detail (29). Crystals of oxide which were oriented to the metal structure were more stable thermodynamically than the unoriented crystallites of the oxide. Given sufficient time the unoriented crystallites gradually formed oriented crystallites. Whatever the mechanism of this reaction, a rather high energy barrier tended to prevent this from occurring. The tendency to form oriented films was aided by increasing the temperature and holding for long periods of time in vacuo.

In the presence of a H_2O-H_2 mixture it is probable that the H_2 may reduce the thermodynamically less stable unoriented crystallites leaving the oriented ones to grow by oxidation with the H_2O. In this manner a highly oriented film of "FeO" can be formed.

There still remains the problem of explaining the results of Nelson (31) on oriented evaporated films of iron. It would appear that the only important difference between the experiments is that the size of the iron crystals in evaporated films is smaller than those used in this study. The role of the crystal size has not been considered in this paper.

Directing Influence of the Metal Substrate Crystal Structure

Bénard (30) suggested two rules for the directing influence of crystal structures in oxidation reaction: (*a*) the oxide tends to orient itself to the metal structure to produce as near a coincidence as possible of the repeat distances between the metal atoms in the two structures, and (*b*) planes of high atomic density in the oxide tend to orient to high density atomic planes in the metal consistent with the geometry of the two structures.

In the oxidation of iron, the diagonal distance across the body-centered iron cube is of length $a_0\sqrt{2}$ or 4.04 Å. Upon this direction the cube direction of "FeO" tends to grow of length 4.29 Å. The fit is not perfect and thus an element of strain is present at this interface. This agreement indicates that the first rule may be important. The planes of high atomic density in α-Fe are the planes (110) while the planes of maximum density of "FeO" are the planes (111). However, geometrical aspects must also be considered since it is impossible to bring into coincidence by a single rotation the 4(110) planes of α-Fe with the 4(111) planes of "FeO." The more feasible arrangement is the parallelism of the (110) planes of α-Fe with the (100) planes of "FeO."

Summary

Orientation of oxide films and scales formed on single crystals of pure iron was studied using the high-temperature electron diffraction reflection camera. Effects of the nature of the oxidizing atmosphere, temperature, time, pressure and surface preparation were considered. The three prominent surface planes, (100), (211), and (311), found in the strain-annealed preparations from rolled Puron strip are used as specimens.

Oxidation in H_2O-H_2 mixtures at 650 and 750°C showed highly oriented films of "FeO" for all three planes (100), (211), and (311). In each case the [010] direction of "FeO" was found to grow in the [110] direction of α-Fe.

Oxidation in H_2O-H_2 mixtures at 300 to 500°C produced highly oriented films of Fe_3O_4 for all three planes (100), (211), and (311). Orientation relationships with the α-Fe crystal surface were the same as found for "FeO."

A study of the forward and reverse transformations following the equation $Fe_3O_4 + Fe \rightarrow 4$"FeO" showed that the orientation relationships are conserved and at no time is the high degree of orientation lost in either the forward or reverse reactions. This would indicate a very close similarity in structure between the "FeO" and Fe_3O_4.

Oxidation in vacuo of the order of 10^{-5} mm of Hg showed a number of interesting features. During the first heating cycle and below 500°C the cross array of spots corresponding to the metal showed long tails rather than the normal spots. This was associated with the extremely thin oxide film. Thicker films showed randomly oriented patterns of either Fe_3O_4 or "FeO" depending upon the temperature although one or two spots were observed. Long heating in vacuo combined with heating and cooling cycles gradually developed a small degree of orientation. However, the process was an extremely slow one compared to the use of H_2O-H_2 mixtures.

Oxidation of specimens in oxygen at 600°C showed that a randomly oriented oxide film is formed. However, if an oriented layer of "FeO" is first formed in H_2O-H_2 mixtures, the oxide rapidly takes on the orientation of the original "FeO" layer.

A study is made of the orientation relationships occurring in the solid phase reactions

$$4\alpha\text{-}Fe_2O_3 + Fe \rightarrow 3Fe_3O_4$$

and

$$Fe_3O_4 + Fe \rightarrow 4\text{"FeO."}$$

If the reaction is studied by additional oxidation on an already oriented "FeO" layer the outer layer of the oxide film consists of nearly randomly oriented α-Fe_2O_3. After a period of time the orienting influence of the "FeO" layer is seen and in a period of ten minutes at 750°C the pattern shows a highly oriented layer of "FeO." The newly formed "FeO" takes on the original highly oriented structure of the "FeO."

The orientation relationships observed are discussed in terms of the directing influence of one structure on another, according to conservation of atomic spacings and the conservation of high atomic density planes.

Any discussion of this paper will appear in a Discussion Section, to be published in the June 1953 issue of the Journal.

References

1. M. L. Royer, *Bull. soc. franç. minéral.*, **51**, 7 (1928).
2. R. F. Mehl and E. L. McCandless, *Trans. Am. Inst. Mining Met. Engrs.*, **125**, 531 (1937).
3. W. G. Burgers and J. J. A. Ploos Van Amstel, *Physica*, **3**, 1056 (1936).
4. W. G. Burgers and H. E. Quanjel, *Rec. trav. chim.*, **61**, 353 (1942).
5. G. I. Finch and A. G. Quarrell, *Proc. Phys. Soc. (London)*, **46**, 148 (1934).
6. W. G. Burgers and J. J. A. Ploos Van Amstel, *Physica*, **3**, 1064 (1936).
7. G. I. Finch, A. G. Quarrell, and H. Wilman, *Trans. Faraday Soc.*, **31**, 1051 (1935).
8. E. Belwe, *Z. Physik*, **100**, 192 (1936) (see Fig. 2).

9. E. A. Gulbransen and J. W. Hickman, *Trans. Am. Inst. Mining Met. Engrs.*, **171**, 306 (1947).
10. R. F. Mehl, E. L. McCandless, and F. N. Rhines, *Nature*, **134**, 1009 (1934).
11. G. D. Preston and L. L. Bircumshaw, *Phil. Mag.*, **20**, 706 (1935).
12. P. A. Thyssen and H. Schutza, *Z. anorg. u. allgem. Chem.*, **233**, 35 (1937).
13. G. P. Thomson, *Proc. Roy. Soc. (London)*, **A133**, 1 (1931).
14. W. L. Bragg, *Nature*, **124**, 125 (1929).
15. W. L. Bragg and F. Kirchner, *Nature*, **127**, 738 (1931).
16. L. H. Germer, *Phys. Rev.*, **44**, 1012 (1933).
17. C. S. Barrett, "Structure of Metals," McGraw-Hill Publishing Co., New York (1943).
18. F. Kirchner, *Ann. Physik*, **13**, 38 (1932).
19. J. A. Darbyshire and E. R. Cooper, *Proc. Roy. Soc. (London)*, **A152**, 104 (1935).
20. L. H. Germer, *Phys. Rev.*, **50**, 659 (1936).
21. G. Menzer, *Ann. Physik*, **36**, 239 (1939).
22. M. J. Buerger, "X-Ray Crystallography," John Wiley & Sons, Inc., New York (1942).
23. J. D. Bernal, *Proc. Roy. Soc. (London)*, **A113**, 117 (1926).
24. P. H. Emmett and J. F. Schultz, *J. Am. Chem. Soc.*, **52**, 4268 (1930).
25. E. A. Gulbransen, *J. Applied Phys.*, **16**, 718 (1945).
26. E. A. Gulbransen, *Rev. Sci. Instruments*, **18**, 546 (1947).
27. E. A. Gulbransen and R. Ruka, *Ind. Eng. Chem.*, **43**, 697 (1951).
28. H. J. Goldschmidt, *J. Iron Steel Inst. (London)*, **146**, 157 (1942).
29. R. T. Phelps, E. A. Gulbransen, and J. W. Hickman, *Ind. Eng. Chem., Anal. Ed.*, **18**, 391 (1946).
30. J. Bénard, *Bull. soc. chim. France*, **13**, 511 (1946).
31. H. R. Nelson, *Nature*, **139**, 30 (1937).
32. J. J. Trillat and S. Oketani, *Compt. rend.*, **230**, 2203 (1950).